Naval Command,
Control and Ocean
Surveillance Center RDT&E Division San Diego, CA
92152-5001

4

Technical Report 1621
September 1993

An Inverse DWT for Nonorthogonal Wavelets

M. J. Shensa

Technical Report 1621
September 1993

An Inverse DWT for Nonorthogonal Wavelets

M. J. Shensa

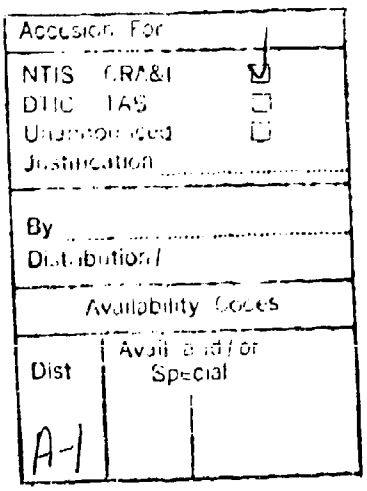

NAVAL COMMAND, CONTROL AND OCEAN SURVEILLANCE CENTER
RDT&E DIVISION
San Diego, California 92152–5001

K. E. EVANS, CAPT, USN
Commanding Officer

R. T. SHEARER
Executive Director

ADMINISTRATIVE INFORMATION

This work was accomplished by the author in the Systems Design Branch (Code 782) of the Naval Command, Control and Ocean Surveillance Center (NCCOSC), Research, Development, Test and Evaluation Division (RDT&E Division). Sponsorship was provided by the Office of Naval Research and the Independent Research and Independent Exploratory Development Programs under program element 0601153N.

Released by
R. A. Dukelow, Head
Systems Design Branch

Under authority of
P. M. Reeves, Head
Analysis and Simulation
Division

PK

CONTENTS

FIGURES

TABLES

I. INTRODUCTION

Nonorthogonal wavelet transforms play an important role in signal processing by offering much greater flexibility in the choice of waveform than their orthogonal counterparts. In particular, they allow adjustment of the relative resolution in time and scale. For example, decreasing the parameter β in the Morlet wavelet $\psi(t) = e^{i\pi t} e^{-\beta^2 t^2/2}$ increases frequency resolution while decreasing time resolution (cf. [1], [2], Appendix A). We are concerned with discrete transforms, however, and increased resolution does little good unless it is accompanied by a sufficiently fine output grid. Such output requires an undecimated transform and the addition of voices (i.e., suboctave sampling), which is generally inconsistent with orthogonality.[1] Moreover, many applications require this finer sampling even when the shape of a relatively broadband mother wavelet is adequate.

The standard inversion procedure for discrete nonorthogonal transforms is a finite expansion in terms of the analyzing wavelet [1], [3], [4]. Formally, it is based on the theory of frames and can be thought of as a a discretization of the corresponding continuous inversion formula. From this point of view, several approximations are involved: the wavelet coefficients themselves, the partial sum, and the use of the analyzing wavelets rather than their duals. While a partial expansion works quite well for many (sufficiently oscillatory) signals, it fails to achieve good accuracy or requires an excessive number of scales for others. Unfortunately, the analyses found in the literature focus on frame bounds rather than the quality of finite discrete implementations, and generally only treat relatively broadband wavelets (i.e., β about 2/3). In short, there is a clear need for a more careful examination of the invertibility of these transforms. This paper provides several alternative algorithms for inversion of the discrete wavelet transform and compares them in the case of Morlet wavelets. In the process, both practical and theoretical issues for the inversion of nonorthogonal discrete wavelet transforms are discussed.

Our ultimate goal is to formulate the problem in an entirely discrete context, unifying the various inverses under a common filter bank structure. The continuous case shall serve as guide and interpreter. The remainder of the introduction is devoted to elaborating this point of view. Section II formally introduces our notation, and Section III describes the dual wavelets in a general setting, providing some results particular to undecimated transforms. Section IV discretizes the continuous case. Section V begins with a general treatment of the discrete inverse wavelet transform including a discussion of appropriate filter constraints. Then, three particularly relevant inverses are presented and analyzed. Section VI provides a numerical comparison of the three inverses and the frame approximation.

[1] This statement is no longer true if one admits bases generated by more than one mother wavelet. Wavelet packets also present a means of obtaining higher resolution. These methods suffer various drawbacks, however, which are outside the scope of this paper.

Let $\psi(t)$ be a square integrable function satisfying the admissibility condition

$$C_\psi \triangleq \int_{-\infty}^{\infty} \frac{|\widehat{\psi}(\omega)|^2}{|\omega|}\, d\omega < \infty \ , \tag{1.1}$$

where

$$\widehat{\psi}(\omega) \triangleq \int \psi(t)\ e^{-j\omega t} \tag{1.2}$$

is the Fourier transform of $\psi(t)$. We define the continuous wavelet transform of a signal s(t) by

$$W(a,\ b) \triangleq \frac{1}{\sqrt{a}} \int s(t)\, \overline{\psi}\left(\frac{t-b}{a}\right)\, dt \ , \tag{1.3}$$

where the bar indicates complex conjugate. For orthonormal wavelets, the following expansion is valid:

$$\begin{aligned} s(t) &= \sum_{i,n} W(2^i, 2^i n) \frac{1}{\sqrt{2^i}}\, \psi\left(\frac{t}{2^i} - n\right) \\ &\triangleq \sum_{i,n} W_{i,n}\, \psi_{i,n} \ . \end{aligned} \tag{1.4}$$

One might hope for a similar expansion for nonorthogonal wavelets. Let us consider discretizing the continuous case. If $\psi(t)$ is real or analytic and satisfies (1.1), then the signal may be recovered by the standard inversion formula [1], [3][2]

$$s(t) = \frac{2}{C_\psi}\, Re \int_0^\infty \frac{da}{a^2} \int_{-\infty}^{\infty} db\ W(a,b)\, \frac{1}{\sqrt{a}}\, \psi\left(\frac{t-b}{a}\right) \ . \tag{1.5}$$

Setting $a = 2^i$ and $b = 2^i n$ in (1.5), we obtain (cf. Section IV)

$$s(t) \approx \frac{2 \ln 2}{C_\psi}\, Re \sum_{i,n} W(2^i, 2^i n)\, \psi\left(\frac{t}{2^i} - n\right) \ , \tag{1.6}$$

which is essentially the same expansion as (1.4). Unfortunately (1.6) is not, in general, correct. The theory of frames [3]–[4] tells us that

$$s(t) = Re \sum_{i,n} W_{i,n}\, \widetilde{\psi_{i,n}}(t) \ , \tag{1.7}$$

---

[2] If $\widehat{\psi}(\omega) = 0$ for $\omega < 0$, then the formula is valid for complex ψ provided one takes the real part as indicated. For all practical purposes, this is the case for Morlet wavelets, $\psi(t) = e^{i\pi t}\, e^{-\beta^2 t^2/2}$, which satisfy $\beta \leq 1/2$ (cf. [1]–[3], Appendix A). Note the limits of the integral in definition (1.1). Some references use 0 to ∞. We prefer (1.1) because it results in the same formulae for both real and analytic wavelets.

where the $\widetilde{\psi_{i,n}}$ are the so-called duals of the $\psi(2^{-i}t - n)$. Nevertheless, under propitious circumstances the wavelets themselves offer a good approximation to the duals. One way to improve this approximation is to add voices; i.e., discretize a at smaller intervals ($a = \gamma^i$, where $1 < \gamma < 2$) [3]. This technique has been highly successful in many applications [5]; however, as hinted above, it is not sufficient to provide a good inverse for narrowband wavelets [6].

If we are to study the situation, we must be able to define the duals or at least make their roles more precise. In this introduction, to simplify the presentation, we avoid defining the functions themselves. Rather, we broach the subject from the point of view of matrices and their pseudo-inverses. There is an additional reason for doing this. Namely, these concepts are particularly appropriate to discrete, finite implementations. Moreover, as with the wavelets themselves, there is rarely a need to actually compute the dual functions; we are only interested in the wavelet coefficients and the inverse algorithm. Let $w_{i,n}$ be the decimated discrete wavelet transform, that is, the discrete analogue of $W(2^i, 2^i n)$. It is defined by

$$\mathbf{s}_{i+1} = \downarrow (\boldsymbol{f} * \mathbf{s}_i) \tag{1.8a}$$

$$\mathbf{w}_i = \boldsymbol{g} * \mathbf{s}_i \tag{1.8b}$$

where $[\mathbf{s}_0]_n = s(n)$ is the discrete signal, $\boldsymbol{f}$ and $\boldsymbol{g}$ are discrete filters, and $\downarrow$ is the decimation (downsampling) operator

$$[\downarrow h]_n = h_{2n} \tag{1.9}$$

One should visualize $g_n = \overline{\psi}(-n)$ as the sampled wavelet and $\boldsymbol{f}$ as a, somewhat arbitrary, interpolation filter [2]. We shall not dwell on regularity questions or the choice of the filters; however, we remark that $\boldsymbol{f}$ must at least satisfy the condition

$$\sum_n f_n = \sqrt{2} \ . \tag{1.10}$$

The reader is referred to the literature [2]-[3]. The recursion (1.8) is easily implemented by the filter bank of figure 1. Ultimately our inverses shall be based on the undecimated discrete wavelet transform (DWT). It corresponds to $W(2^i, n)$ and is illustrated in figure 2a. Denoted w_n^i, this transform satisfies $\mathrm{w}_{2^i n}^i = w_{i,n}$ [2]. It is more appropriate to most applications of nonorthogonal wavelets where, as we have mentioned, output resolution is an issue. Moreover, the undecimated transform provides a better basis for recovering the signal s(n).

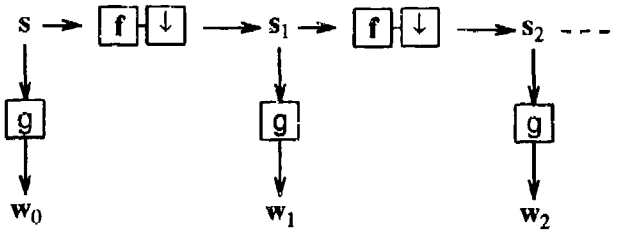

Figure 1. A wavelet filter bank structure implementing the decimated discrete wavelet transform. The down-arrow indicates decimation. The output of the transform is the family of vectors w_i, forming the two parameter transform $w_{i,n}$ in the scale-time plane.

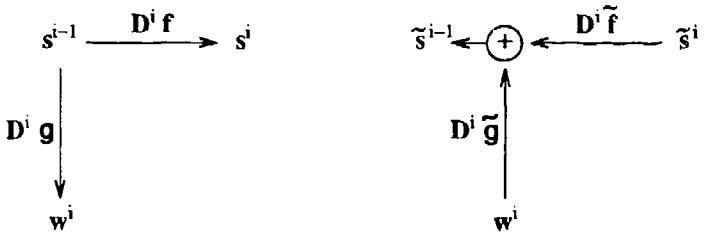

(a) DWT (b) DWT^{-1}

Figure 2. One stage of (a) the undecimated discrete wavelet transform, and (b) of the inverse discrete wavelet transform. $\mathbf{s}^0$ is the input signal and the "initial" stage of DWT^{-1} is determined by $\tilde{s}^M = s^M$. $\mathbf{D}^i \boldsymbol{f}$ is the filter obtained from $\boldsymbol{f}$ by inserting $2^i - 1$ zeros between its elements.

Suppose there are M stages[3] to the DWT; i.e., $i = 0, \ldots, M-1$. Then, the DWT maps $\mathbb{R}$ into $\mathbb{R}^{M+1}$

$$\mathbf{s} \stackrel{DWT}{\longrightarrow} \{\mathbf{w}^i : i = 0, \ldots, M-1 \,;\, \mathbf{s}^M\} \ . \tag{1.11}$$

Under very weak regularity conditions, the norm of $\mathbf{s}^M$ goes to zero as M goes to ∞ (see Appendix B). However, in order for the transformation to be nonsingular for finite M, one must include the smoothed signal $\mathbf{s}^M$ as well as the wavelet coefficients $\mathbf{w}^i$. This transformation is clearly linear (although not time invariant in the decimated case) and may be represented by a matrix $\mathbf{A}$. If $\boldsymbol{f}$ and $\boldsymbol{g}$ are finite, the transformation is locally finite (each row of $\mathbf{A}$ is zero except for a section of fixed length); but, the matrix itself

[3] That is, so-called scales or octaves. In general, one will also have several voices. See Section IV

is infinite because the convolution acts on arbitrarily long signals. Also, the image of the transformation is a proper subset of $\mathbb{R}^{M+1}$ so that a true inverse does not exist. Nonetheless, it is generally injective so that $\mathbf{A}^\dagger\mathbf{A}$ is nonsingular, and we may "invert" objects in the range space $\mathbb{R}^{M+1}$ by using the pseudo-inverse

$$\mathbf{P} \triangleq (\mathbf{A}^\dagger\mathbf{A})^{-1}\mathbf{A}^\dagger \tag{1.12}$$

where $[\mathbf{A}^\dagger]_{i,j} = \overline{\mathbf{A}_{j,i}}$. It is trivial to verify that $\mathbf{PA} = \mathbf{I}$. On the other hand, $\mathbf{AP} \neq \mathbf{I}$.

There are many other matrices $\mathbf{Q}$ which have the property $\mathbf{QA} = \mathbf{I}$. In fact, if $\mathbf{B}$ is any matrix such that $\mathbf{BA}$ is nonsingular, then

$$\mathbf{Q} = (\mathbf{BA})^{-1}\mathbf{B} \tag{1.13}$$

satisfies such a relation. The pseudo-inverse is unique inasmuch as it is an orthogonal projection of $\mathbb{R}^{M+1}$ onto the image of the DWT. For example, suppose one were to filter the wavelet transform (possibly stepping outside of its range) and invert it

$$\mathbf{w} \xrightarrow{filter} \mathbf{h} \in \mathbb{R}^{M+1} \xrightarrow{\mathbf{Q}} \mathbf{r} \xrightarrow{DWT} \mathbf{Ar} \ .$$

Then, in general, $\mathbf{Ar} \neq \mathbf{h}$, but the pseudo-inverse minimizes the squared error $\|\mathbf{h}-\mathbf{Ar}\|^2 = \|\mathbf{h}-\mathbf{AQh}\|^2$ among all possible $\mathbf{Q}$. Note that this holds for non-Euclidean metrics on $\mathbb{R}^{M+1}$ provided $\mathbf{A}^\dagger$ is replaced by the adjoint transformation relative to the metric. Although the pseudo-inverse is a natural choice, other issues are involved. Often the error criterion is not a metric on $\mathbb{R}^{M+1}$, or computational complexity is an important consideration.

An alternative approach is to invert a single stage of the DWT, thereby inverting the entire transform. For the undecimated DWT, it suffices to find filters $\widetilde{f}$ and $\widetilde{g}$ such that

$$\widetilde{f} * f + \widetilde{g} * g = \delta \ , \tag{1.14}$$

where $[\delta]_m = \delta_{0,m}$ is the Kronecker delta. More precisely, if $\mathbf{D}^i$ is the operator which inserts $2^i - 1$ zeros between the elements of a vector, then $\mathbf{D}^i(f * g) = \mathbf{D}^i f * \mathbf{D}^i g$. It follows that (1.14) is equivalent to

$$(\mathbf{D}^i\widetilde{f}) * (\mathbf{D}^i f) + (\mathbf{D}^i\widetilde{g}) * (\mathbf{D}^i g) = \delta \ . \tag{1.15}$$

Thus, under (1.14), the inverse filterbank of figure 2b is a left inverse for the DWT, that is, for figure 2a.

These three points of view (dual expansions, left or pseudo-inverses, and filter banks) begin to merge if one considers a more general class of filters than those satisfying (1.14). The usual inversion procedure for nonorthogonal wavelets is to approximate (1.7) with

$$s(t) \approx Re \sum_{n,\, i=0,\ldots,M-1} \mathrm{w}_{i,n}\widetilde{\psi_{i,n}}(t) \approx constant \cdot Re \sum_{n,\, i=0,\ldots,M-1} \mathrm{w}_{i,n}\psi_{i,n}(t) \ . \tag{1.16}$$

The approximations involved in the traditional frame inverse may then be reinterpreted from a filter bank perspective. The finite sum (i.e., $M < \infty$) is equivalent to ignoring $\mathbf{s^M}$, while the use of the wavelets instead of their duals is tantamount to setting $\mathbf{A^\dagger A} = \mathbf{I}$ in (1.12). Furthermore, if we choose $\widetilde{f}$ and $\widetilde{g}$ to be $\widetilde{f}_n = \overline{f}_{-n}$ and $\widetilde{g}_n = \overline{g}_{-n}$, then the inverse filter bank of figure 2b computes the adjoint transformation $\mathbf{A^\dagger}$ (c.f. Section V). Thus, the inverse filterbank provides a unifying framework from which to study the various inverses. In fact, we shall adopt the terminology inverse discrete wavelet transform or DWT^{-1} [6] to refer to any inverse filter bank whether or not the filters satisfy (1.14). To be useful, the filters should be chosen to provide an approximate left inverse to DWT; however, in general, an exact left inverse will only be achieved with iteration.

There are, of course, tradeoffs which accompany the various approximations. Some of the negative aspects are (a) filters satisfying equation (1.14) are usually prohibitively long (e.g., Morlet wavelets), (b) these filters generally provide inverses which are not the pseudo-inverse, and (c) although $\mathbf{A^\dagger w}$ is readily computed, $\mathbf{(A^\dagger A)^{-1} A^\dagger w}$ is not. We find, however, in the context of inverse filter banks, that these problems may be successfully evaded. First, let us note that if a true left inverse is desired, it may be computed at a very moderate computational cost simply by iterating (so-called Neumann inverse) the forward and reverse transforms of figure 2.[4] In fact, computationally, this technique seems much more effective that than using long filters to achieve comparable accuracy.

Secondly, a number of good approximate inverses exist which are sufficient for many applications without the above iteration. For example, a substantial improvement over (1.16) is obtained, at essentially no cost, by including $\mathbf{s}^M$. Also, just as the inclusion of voices provides redundancy creating a tighter frame and therefore a better inverse [3], the use of undecimated wavelets enables us to find inverses which perform better than (1.16) with considerably less computation.[5] How do we go about finding these inverses? One very effective method which also lends considerable insight is to mimic the continuous case. A more direct approach is to try to invert a single stage; that is, approximate (1.14) using filters which are not too long or satisfy suitable constraints. One must take care, however, to insure that the error does not increase unduly as the inverse passes up the filter bank. It is certainly possible, to find cases in which some degradation of the single stage approximation actually improves the performance over a cascade of several stages. It may also be preferable to use a coarse approximation and then iterate. We can argue, however, that if the inverse is to be applied to an unspecified class of signals and operate with little or no iteration, then, a single iteration of a one-octave transform must give a good inverse; i.e., the single stage inverse must be acceptable.

---

[4] In general, any nonsingular inverse filterbank is a linear transformation $\mathbf{B}$ which may be iterated in conjunction with the forward transform to compute a left inverse $\mathbf{Q}$ defined by (1.13).

[5] One even finds that the duals to the undecimated wavelets may be computed (if for some strange reason one wishes to do so) more efficiently since they are translation invariant rather than scale invariant as in the decimated case (cf. Section III).

II. DEFINITIONS AND NOTATION

A major notational distinction is the use of superscripts for undecimated entities versus subscripts when they are decimated. We define the standard families of wavelet functions generated from the mother wavelet ψ by

$$\psi_n^i(t) \triangleq \frac{1}{\sqrt{2^i}}\,\psi\left(\frac{t-n}{2^i}\right) \tag{2.1a}$$

$$\psi_{i,n}(t) \triangleq \frac{1}{\sqrt{2^i}}\,\psi\left(\frac{t}{2^i}-n\right) \quad . \tag{2.1b}$$

The corresponding sampled continuous wavelet transforms are given by

$$W_n^i \triangleq \int s(\tau)\,\overline{\psi}_n^i(\tau)\,d\tau \;=\; <s,\psi_n^i> \tag{2.2a}$$

$$W_{i,n} \triangleq \int s(\tau)\,\overline{\psi}_{i,n}(\tau)\,d\tau \;=\; <s,\psi_{i,n}> \quad . \tag{2.2b}$$

This notation differs slightly from [3] which uses $\psi^{i,n}$; however, it enables us to treat the discrete transforms as vectors; i.e., $\mathrm{w}_n^i = [\mathbf{w}^i]_n$. Unless specified to be otherwise, norms are assumed to be L^2 for functions, $\|\psi\|^2 = <\psi,\psi>$, and l^2 for vectors, $\|\mathbf{w}\|^2 = \sum_n(\mathrm{w_n})^2$. Finally, let us remark that additional voices are indicated by ψ_n^{iv} and $\psi_{iv,n}$, which are equivalent to (2.1a) and (2.1b) respectively with 2^i replaced by $2^i \cdot 2^{v/L}$ where L is the number of voices. More formal definitions are postponed to Section IV where voices will be treated in detail.

For our purposes, W_i and W^i serve mainly as an aids in the interpretation of the corresponding discrete wavelet transforms. These discrete transforms, $\mathrm{w}_{i,n}$ and w_n^i, may be computed according to the diagrams of figures 1 and 2a respectively. The former is defined by equations (1.8); the latter is defined as follows: Let $\mathbf{D}^i$ be the dilation operator that inserts $2^i - 1$ zeros between each of the elements of a vector; i.e.,

$$[\mathbf{D}^i \boldsymbol{f}]_{2^i k+r} \triangleq \begin{cases} f_k, & \text{for } r = 0 \\ 0, & \text{otherwise} \end{cases} \quad . \tag{2.3}$$

For a given lowpass filter $\boldsymbol{f}$ and highpass filter $\boldsymbol{g}$, the undecimated DWT is determined by the following recursion [2]

$$\mathbf{s}^{i+1} \;=\; \mathbf{D}^i \boldsymbol{f} * \mathbf{s}^i \tag{2.4a}$$

$$\mathbf{w}^i \;=\; \mathbf{D}^i \boldsymbol{g} * \mathbf{s}^i \tag{2.4b}$$

with $[\mathbf{s}^0]_n \;=\; s(n)$, the discretized signal. The filter $\boldsymbol{g}$ is generally determined by sampling the mother wavelet; that is,

$$[\boldsymbol{g}]_n \triangleq \overline{\psi}(-n) \tag{2.5}$$

The relationship between the two transforms may be expressed by

$$\mathrm{w}_{i,n} \;=\; \mathrm{w}^{i}_{2^i n} \;. \tag{2.6}$$

We make the standard observation that the ψ^i_n are translation invariant

$$\psi^i_n \;=\; [\psi^i]_n \;\triangleq\; \psi^i(t-n) \;\triangleq\; \psi\left(\frac{t-n}{2^i}\right) \;, \tag{2.7a}$$

while the $\psi_{i,n}$ are not

$$\psi_{i,n} \;=\; \psi\left(\frac{t}{2^i}-n\right) \;\neq\; \psi^i(t-n) \;. \tag{2.7b}$$

Similarly, let $\mathbf{T}_m$ be the operation of translation by m; i.e.,

$$[\mathbf{T}_m \mathbf{s}]_n \;\triangleq\; \mathbf{s}_{n-m} \;, \tag{2.8}$$

and introduce a vector argument s to $\mathbf{w}^i$ to indicate dependence on the signal. It follows immediately from equations (2.4) that the undecimated wavelet transform is translation invariant, i.e.,

$$\mathrm{w}^i_{n+m}(\mathbf{s}) \;=\; \mathrm{w}^i_n(\mathbf{T}_{-m}\mathbf{s}) \;. \tag{2.9}$$

On the other hand, as a consequence of the downsampling in (1.8), the $\mathrm{w}_{i,n}$ are not.

We shall use a tilde to denote the dual wavelets. This operator

$$\widetilde{\psi_{i,n}} \;=\; (\psi_{i,n})\tilde{} \tag{2.10}$$

depends on the structure of the entire family of $\{\psi_{j,m}\}$, not just on the single function $\psi_{i,n}$. As a consequence the translates (dilates) of the dual wavelets are not necessarily the duals of translations (dilations) of the wavelets. That is, the dual operator does not always commute with translation and/or scaling. In particular, although $\psi_{0,0}(t) = \psi^0_0(t) = \psi(t)$, we have the bizarre effect that

$$\widetilde{\psi_{0,0}}(t) \;\neq\; \widetilde{\psi^0_0}(t) \;, \tag{2.11}$$

and, in fact, $\widetilde{\psi}(t)$ makes no sense at all. We stretch the notation by also using tilde to denote the filters of the inverse filter bank, e.g., $\widetilde{f}$ and $\widetilde{g}$. The idea is that, just as the forward filters are associated with the wavelets, the inverse filters are, at least conceptually, associated with the dual wavelets.

The operator † has several (consistent) interpretations depending on the context. For matrices, it denotes the adjoint

$$[\mathbf{A}^\dagger]_{ij} \;\triangleq\; [\overline{\mathbf{A}}]_{ji} \;. \tag{2.12a}$$

For vectors, it is the complex time reversal

$$[f^\dagger]_i \;\triangleq\; [\overline{f}]_{-i} \;, \tag{2.12b}$$

which is consistent with the adjoint of the matrix corresponding to convolution by f; that is, with respect to a matrix $[\mathbf{F}]_{i,j} \triangleq f_{i-j}$ where $f * \mathbf{s} = \mathbf{F}\mathbf{s}$. More generally, $\mathbf{A}^\dagger$ represents the adjoint of an operator in a Hilbert space with inner product $<\cdot, \cdot>$

$$<\mathbf{A}^\dagger \mathbf{x}, \mathbf{x}> \; = \; <\mathbf{x}, \mathbf{A}\mathbf{x}>, \tag{2.12c}$$

which, under the Euclidean metric, agrees with the matrix adjoint. Finally, we shall have some occasion to use the z-transform. It is defined, on the unit circle, by

$$f_z(\omega) \triangleq \sum_n f_n e^{-i\omega n}, \tag{2.13}$$

which agrees with the Fourier transform defined in (1.2). Note that

$$(\mathbf{D}^i f)_z(\omega) \; = \; f_z(2^i \omega) \; . \tag{2.14}$$

III. PROPERTIES OF THE DUALS

In this section, we define the dual wavelets, relate them to the pseudo-inverse, and derive their properties under translation and scaling. We demonstrate that, unlike the duals of the decimated wavelets (cf. [3]), undecimated wavelets have duals which are translation invariant. The unmathematical reader may, without loss of continuity, shun all but subsection III.B and simply consider the dual wavelets to be an arbitrary family of functions $\widetilde{\psi_{i,m}}$ that provide the inverse expansion $s(t) = \sum_{i,n} W_{i,n}\widetilde{\psi_{i,n}}(t) = \sum_{i,n} <s,\ \psi_{i,n}> \widetilde{\psi_{i,n}}(t)$. With a little more effort, one might wish to keep in mind the following discrete interpretation (cf. Appendix C): Let $\mathbf{A}$ be a matrix representing the discrete wavelet transformation, and $\mathbf{A}^\dagger$ its adjoint. Then, the rows of $\mathbf{A}$ correspond to the frame vectors $\psi_{i,n}$ with k^{th} component $[\psi_{i,n}]_k = \psi_{i,n}(k)$, and the dual vectors $\widetilde{\psi_{i,n}}$ correspond to the columns of $(\mathbf{A}^\dagger\mathbf{A})^{-1}\mathbf{A}^\dagger$ (cf. the pseudo-inverse of equation (1.12)). Note that $\mathbf{A}$ depends on the entire family of wavelets so that, $\widetilde{\psi_{i,n}}$ has a nonlinear dependence on $\psi_{i,n}$. The orthonormal case, where $\mathbf{A}^\dagger\mathbf{A}$ is the identity so that $\psi_{i,n} = \widetilde{\psi_{i,n}}$, is an exception.

For continuous signals and real wavelets, the dual wavelets are given by[6]

$$\widetilde{\psi_{i,n}} \ = \ [(\mathcal{A}_{dec}^{\dagger}\mathcal{A}_{dec})^{-1}\psi]_{i,n} \ , \tag{3.1}$$

where the wavelet transform $\mathcal{A}_{dec}$ is defined by $[\mathcal{A}_{dec}\, s]_{i,n} \ = \ <s,\ \psi_{i,n}>$. The analogous expression is used to define the duals $\widetilde{\psi_n^i}$. Different metrics on the image space produce different adjoints and hence different families of duals and different left inverses. In particular, the standard frame formulation uses a resolution of the identity

$$s \ = \ \sum_{i,n} <s,\ \psi_{i,n}> \widetilde{\psi_{i,n}} \tag{3.2}$$

based on the Euclidean metric for decimated wavelets. That is, it is the pseudo-inverse (1.12) where $\mathcal{A}^\dagger$ is defined relative to the metric $\|\mathbf{w}_{dec}\|^2 = \sum_{i,n} |\mathrm{w}_{i,n}|^2$, and $\widetilde{\psi_{i,n}}$ by (3.1). This metric corresponds to energy since $|\mathrm{w}_{i,n}|^2$ is power per Hz and the cells at octave i have area $(2^i\ sec)(1/2^i\ Hz) = 1$ (see Section IV). Similarly, the energy metric for undecimated wavelets is $\|\mathbf{w}^{undec}\|^2 = \sum_{i,n} 2^{-i} |\mathrm{w}_n^i|^2$, so that, for example, if the decimated wavelets $\psi_{i,n}$ are orthonormal, the undecimated dual wavelets satisfy $\widetilde{\psi_n^i} = 2^{-i}\psi_n^i$ in contrast to $\widetilde{\psi_{i,n}} = \psi_{i,n}$. The energy metric is intuitively pleasing, and for decimated wavelets its pseudo-inverse is an orthogonal projection, so this left inverse is often the one of choice. However, one should not arbitrarily dismiss alternative metrics. First, as we shall

[6] In the case of complex analytic wavelets, a complete set for $L^2(\mathbb{R})$ is given by $\{\psi_j^i,\ \overline{\widetilde{\psi_j^i}}\}$. that is, strictly speaking, the frame expansion involves two mother wavelets ψ and $\overline{\widetilde{\psi}}$. Similarly, the family of duals is $\{\widetilde{\psi_j^i},\ \overline{\psi_j^i}\}$ [4]. Alternatively, for real signals, one may take the real part as in (1.7). This aspect is ignored in this section in order to simplify the presentation.

see in succeeding sections, other left inverses have considerable computational/numerical advantages. Furthermore, it is not a priori clear that alternative metrics may not enhance one's signal processing, at least in particular situations. In fact, every inverse of the form (1.13) corresponds to a pseudo-inverse with respect to an appropriate metric.

We make this more precise. The pseudo-inverse may be characterized as is the unique left inverse such that its null space is orthogonal to the range of the transform. We note that, provided $\mathbf{BA}$ is nonsingular, $\mathbf{Q} = (\mathbf{BA})^{-1}\mathbf{B}$ is a left inverse of $\mathbf{A}$. Also, since $\mathbf{BA}$ is nonsingular, the null space of $\mathbf{Q}$ coincides with the null space of $\mathbf{B}$, and it is easy to see that the range of $\mathbf{A}$ and the null space of $\mathbf{B}$ are disjoint and span the embedding space (i.e., time-scale space). Thus, any vector $\mathbf{w}$ in this space may be written uniquely as the sum of vectors in these two subspaces. For $\mathbf{Q}$ to be the pseudo-inverse, it suffices to chose a metric for which these two spaces are orthogonal. In fact, such a metric is given explicitly by

$$<\mathbf{w}, \mathbf{w}>_B \triangleq \|\mathbf{A}(\mathbf{BA})^{-1}\mathbf{B}\,\mathbf{w}\|^2 + \|(\mathbf{I} - \mathbf{A}(\mathbf{BA})^{-1}\mathbf{B})\,\mathbf{w}\|^2 \ . \tag{3.3}$$

A. Invariance

In [3] it is shown that the duals of the decimated wavelets are scale invariant in the sense that $\widetilde{\psi_{i,n}} = 2^{-i/2}\widetilde{\psi_{0,n}}(t/2^i)$, but that they are not invariant under translation, i.e., $\widetilde{\psi_{i,n}} \neq \widetilde{\psi_{i,0}}(t-n)$. In this section, we show that for undecimated wavelets the reverse is true. That is, their duals are translation invariant but not scale invariant. This is of theoretical interest and also has a certain degree of practical impact. It implies that the undecimated duals may be all computed by determining one function for each octave and then translating. Since there are generally many more time points than there are octaves, this property appears to be more useful than scale invariance.

The forward undecimated wavelet transformation $\mathcal{A}$ may be represented by

$$[\mathcal{A}\,s]^i_n = <s,\ \psi^i_n> \ . \tag{3.4}$$

We then have (with the energy metric)

$$\begin{aligned} <\mathcal{A}^\dagger\mathcal{A}s,\ r> &= <\mathcal{A}s,\ \mathcal{A}r> \\ &= \sum_{i,n} 2^{-i} <s,\ \psi^i_n> <\psi^i_n,\ r> \ , \end{aligned} \tag{3.5}$$

which implies that

$$\mathcal{A}^\dagger\mathcal{A} = \sum_{i,n} 2^{-i} <\cdot,\ \psi^i_n> \psi^i_n \ . \tag{3.6}$$

Next, let us define the scale/time translation operator

$$U^{(a)}_b\, s(t) \triangleq \frac{1}{\sqrt{a}}\, s\left(\frac{t-b}{a}\right) \ . \tag{3.7}$$

Its adjoint is given by

$$[U_b^{(a)}]^\dagger \;=\; U_{-b/a}^{(1/a)} \;, \tag{3.8}$$

which follows from

$$\int (U_b^{(a)} s(t))\, \overline{r(t)}\, dt \;=\; \int \frac{1}{\sqrt{a}}\, s\Big(\Big(\frac{t-b}{a}\Big)\Big)\, \overline{r(t)}\, dt \;=\; \int s(\tau)\, \overline{r(\tau a + b)}\, \sqrt{a}\, d\tau \;. \tag{3.9}$$

Note, that we also have

$$U_{b'}^{(a')}\, U_b^{(a)} \;=\; U_{b'+a'b}^{(aa')} \;. \tag{3.10}$$

We are particularly concerned with the family

$$U_n^i \;\triangleq\; U_n^{(2^i)} \;. \tag{3.11}$$

If $\mathcal{A}^\dagger \mathcal{A}$ commutes with U_n^0 then the family of duals is translation invariant; if it commutes with U_0^i, then the family is scale invariant. For example, commutation of $\mathcal{A}^\dagger \mathcal{A}$ with U_n^0 implies commutation of $(\mathcal{A}^\dagger \mathcal{A})^{-1}$ with U_n^0, and

$$\widetilde{\psi_n^i}(t) \;=\; (\mathcal{A}^\dagger \mathcal{A})^{-1} \psi_n^i \;=\; (\mathcal{A}^\dagger \mathcal{A})^{-1} U_n^0\, \psi_0^i \;=\; U_n^0\, (\mathcal{A}^\dagger \mathcal{A})^{-1}\, \psi_0^i \;=\; \widetilde{\psi_0^i}(t-n) \;. \tag{3.12}$$

Proposition 3.1: Let ψ be any admissible wavelet. Then,

(i) Under any translation invariant metric, the family of dual wavelets for the undecimated discrete wavelet transform is time invariant but not scale invariant; i.e.,

$$\widetilde{\psi_n^i}(t) \;=\; \widetilde{\psi_0^i}(t-n)\;;\;\; \widetilde{\psi_n^i}(t) \;\neq\; 2^{-i/2} \widetilde{\psi_n^0}(t/2^i) \;. \tag{3.13}$$

(ii) Under any scale invariant metric, the family of dual wavelets for the decimated discrete wavelet transform is scale invariant but not time invariant; i.e.,

$$\widetilde{\psi_{i,n}}(t) \;=\; 2^{-i/2} \widetilde{\psi_{0,n}}(t/2^i) \;\; \widetilde{\psi_{i,n}}(t) \;\neq\; \widetilde{\psi_{i,0}}(t-n)\;; \tag{3.14}$$

We remark that, in l^∞, a translation invariant metric $<\mathbf{x},\, \mathbf{y}>_g = \sum_{ijnm} x_n^i g_{nm}^{ij} y_m^j$ is one for which $g_{nm}^{ij} = g_{n+k,m+k}^{ij}$. Scale invariance is defined analogously. For notational clarity, we only prove (i) under the energy metric.

Proof: From (3.6), we compute

$$U_m^j\, \mathcal{A}^\dagger \mathcal{A} \;=\; \sum_{i,n} 2^{-i} <\cdot,\, U_n^i\, \psi> U_m^j\, U_n^i\, \psi \;=\; \sum_{i,n} <\cdot,\, U_n^i\, \psi>\, U_{m+2^j n}^{j+i}\, \psi \;, \tag{3.15}$$

and

$$\begin{aligned}
\mathcal{A}^\dagger \mathcal{A}\, U_m^j \;&=\; \sum_{i,n} 2^{-i} <\cdot,\, {U_m^j}^\dagger\, U_n^i\, \psi>\, U_n^i\, \psi \\
&=\; \sum_{i,n} 2^{-i} <\cdot,\, U_{-2^{-j} m}^{-j}\, U_n^i\, \psi>\, U_n^i\, \psi \\
&=\; \sum_{i,n} 2^{-i} <\cdot,\, U_{2^{-j}(-m+n)}^{i-j}\, \psi>\, U_n^i\, \psi \\
&=\; \sum_{i',n} 2^{-i'-j} <\cdot,\, U_{2^{-j}(-m+n)}^{i'}\, \psi>\, U_n^{j+i'}\, \psi \;.
\end{aligned} \tag{3.16}$$

Even if we accept translation invariance up to a scalar factor 2^{-j}, to equate (3.15) and (3.14) we still need to make the substitution, $n' = 2^{-j}(n-m)$. This is only possible for $j = 0$ since n' must be an integer. In fact, for general ψ, equality occurs only for U_m^0, and not for U_0^j. On the other hand, for decimated wavelets, the operator $\mathcal{A}_{dec}^{\dagger}\mathcal{A}_{dec}$ takes the form $\sum_{i,n} < \cdot, U_{2^i n}^i \psi > U_{2^i n}^i \psi$, and it is easy to confirm that this operator commutes with U_0^j, but not with U_m^0.

B. The Neumann Inverse

Often, given a discrete wavelet transform, $\mathcal{A}$ and an approximate inverse $\mathcal{B}$ (for example, an inverse filter bank DWT^{-1}), we would like to compute an exact left inverse, in particular that of equation (1.13). This may be done by using the Neumann inverse for linear operators[7]

$$\mathcal{S}^{-1} \;=\; \mu \sum_{k=0}^{\infty} (\mathcal{I} - \mu\mathcal{S})^k \tag{3.17}$$

where S is a Hilbert space operator and μ is sufficiently small to insure convergence; that is, $(\|(I - \mu\mathcal{S})\| < 1$ [3], [7]. Equation (1.13) may then be written

$$(\mathcal{B}\mathcal{A})^{-1}\mathcal{B} \;=\; \mu \sum_{k=0}^{\infty} (\mathcal{I} - \mu\mathcal{B}\mathcal{A})^k \mathcal{B} \;. \tag{3.18}$$

The summands in (3.18) can be computed by the recursion $\epsilon_k = \epsilon_{k-1} - \mu\,\mathcal{B}\,\mathcal{A}\epsilon_{i-1}$. Here, $\mathcal{A}$ and $\mathcal{B}$ are the transforms DWT and DWT^{-1}, implemented by filter banks. One may use the following algorithm to compute a true left inverse as accurately as desired.

Algorithm 3.1

(0) $\mathbf{x}_0 = (DWT)^{-1}\mathbf{w}$
$\epsilon_0 = \mathbf{x}_0$

(1) $\epsilon_k \;=\; \epsilon_{k-1} - \mu\, DWT^{-1} \circ DWT\, \epsilon_{k-1}$

(2) $\mathbf{x}_k \;=\; \mathbf{x}_{k-1} \;+\; \epsilon_k$

(3) $leftinverse(k) \;=\; \mu\, \mathbf{x}_k$
go to (1)

A computational drawback that becomes apparent, upon applying Algorithm 3.1, is the huge increase in the signal's support (length) under the mapping $DWT^{-1} \circ DWT$. In fact, if a filter $\boldsymbol{g}$ has length r then $\mathbf{D}^i\boldsymbol{g}$ has length $(2^i - 1)(r-1) + r$, and $(\mathbf{D}^i\boldsymbol{g}) * \mathbf{s}^i$ adds $(2^i - 1)(r-1)$ points to the support of $\mathbf{s}^i$. There is an additional effect due to $\mathbf{D}^i\boldsymbol{f}$, although for Morlet wavelets $\boldsymbol{g}$ is much longer than $\boldsymbol{f}$ and, hence, dominates the problem.

[7] This formula is easily understood, if we replace the linear operator S by a scalar s, let $x = 1 - \mu s$, and consider the expansion $s^{-1} = \mu/(1-x) = \mu \sum_{k=0}^{\infty} x^k$.

The same comments hold true for DWT^{-1}. For example, for five octaves and $r = 50$, the time series $DWT \circ DWT^{-1}\mathbf{w}$ will be about 3000 samples (2 x 31 x 49) longer than $\mathbf{w}$. Each iteration of Algorithm 3.1 adds such an amount to the support of $\mathbf{x}_k$. Clearly, this is unsupportable. Fortunately, the obvious heuristic solution, clipping the support of the iterations, works and can be justified. Let $\mathcal{H}_\mathbf{w}$ be the operator

$$(\mathcal{H}_\mathbf{w}\ \mathbf{y})^i_n\ =\ \begin{cases} \mathbf{y}^i_n, & \text{for } (i,n) \text{ in the support of } \mathbf{w} \\ 0, & \text{otherwise} \end{cases} . \tag{3.19}$$

We simply replace DWT^{-1} in step (1) of Algorithm 3.1 by $\mathcal{H}_\mathbf{w} \circ DWT^{-1}$. That is, we set $DWT\,\epsilon_k$ to zero outside of the support of $\mathbf{w}$. This is equivalent to replacing $\mathcal{B}$ in (3.18) by $\mathcal{B}' = \mathcal{H}_\mathbf{w}\,\mathcal{B}$, and leads to a valid left inverse provided μ is small enough and $\mathcal{B}'\mathcal{A}$ is nonsingular. Because of the w-dependent clipping, this inverse is actually nonlinear. Of course, one could always create a similar, but linear, operator by restricting oneself to a family of signals with fixed support.

IV. APPROXIMATIONS TO CONTINUOUS INVERSES

Of course, (1.5) is not the only continuous inverse. As with the wavelet series, there is an infinity of left inverses for the continuous wavelet transform. In this section, we examine two of these. The results shall be used in Section V as guidelines for inversion where they provide discrete metrics and appropriate filter normalizations for the DWT^{-1}. In the presence of voices these normalizations become nontrivial and extremely confusing; however, they are essential for correct implementation of the inverse transform.

A. *Double-integral inverse (resolution of identity)*

We begin with (1.5), which for convenience we rewrite as

$$s(t) = Re\,\frac{2}{C_\psi}\int \frac{da\,db}{a^2}\,W_b^a\,\psi_b^a(t) \tag{4.1}$$

where

$$\psi_b^a(t) \triangleq \frac{1}{\sqrt{a}}\,\psi\left(\frac{t-b}{a}\right) \quad . \tag{4.2}$$

Recall that s is real, ψ must be real or analytic ($\widehat{\psi}(\omega) = 0$ for $\omega < 0$), a is nonnegative, and Re denotes the real part. The wavelet transforms themselves are generally complex. For simplicity, we shall sometimes drop the Re. Also, observe that a factor $1/\sqrt{a}$ is included in the definition of the wavelet $\psi_b^a(t)$. As a result the L^2 norm of ψ_b^a is independent of a and b. It often helps conceptually to normalize the mother wavelet, $\|\psi\|^2 = 1$. Alternatively, the norm of ψ may be absorbed in the constant C_ψ (cf. equation (1.1)).

Let us discretize the integral and compare it to the sum (1.7). The coefficients W_b^a are given for for all integral values of b in the undecimated case and for $b = 2^i$ in the decimated case. This results in $db \approx \Delta b = 1$ and $db \approx 2^i$ respectively. When the scales are output by octaves, a takes on the values $a = 2^i$ for integer i. Thus, $da/a = d(\ln a) \approx \Delta(i \ln 2) = \ln 2$. Substituting these expressions into (4.1) yields

$$s(t) \;\approx\; Re\,\frac{2\ln 2}{C_\psi}\sum_{i,n} W_n^i\,\frac{1}{2^i}\psi_n^i(t) \tag{4.3a}$$

for the undecimated wavelets, and

$$s(t) \;\approx\; Re\,\frac{2\ln 2}{C_\psi}\sum_{i,n} W_{i,n}\,\psi_{i,n}(t) \tag{4.3b}$$

for the decimated wavelets since $\Delta b = 2^i$ cancels the factor in the denominator. Comparing these with (1.7) and its undecimated equivalent, we see that

$$\widetilde{\psi_n^i} \;\approx\; \frac{2\ln 2}{C_\psi}\,\frac{1}{2^i}\,\psi_n^i \tag{4.4a}$$

$$\widetilde{\psi_{i,n}} \approx \frac{2\ln 2}{C_\psi}\,\psi_{i,n} \ . \tag{4.4b}$$

Note that (4.4b) agrees with (1.16) and that both the expressions (4.4a) and (4.4b) are exact when the $\psi_{i,n}$ form an orthonormal basis [3].

However, we are interested in nonorthogonal wavelets, which, in general, require a finer output grid, that is, voices. If each octave is divided into L voices, we have

$$a \triangleq 2^i\gamma^v \triangleq 2^{i+(v/L)} \ , \tag{4.5}$$

where $i = 0, \ldots M-1$; $v = 0, \ldots L-1$; and

$$\gamma \triangleq 2^{1/L} \ . \tag{4.6}$$

Substituting (4.5) into (4.2) yields

$$\psi_n^{iv} = \frac{1}{\sqrt{2^i\gamma^v}}\,\psi\left(\frac{t-n}{2^i\gamma^v}\right) \ , \tag{4.7}$$

with a similar expression, $\psi_{iv,n} = 2^{-i/2}\gamma^{-v/2}\,\psi(2^{-i}\gamma^{-v}t - n)$, for decimated wavelets. Voices for the discrete transform are usually computed by replicating the filter bank with a new mother wavelet

$$\psi^v(t) \triangleq \frac{1}{\sqrt{\gamma^v}}\,\psi\left(\frac{t}{\gamma^v}\right) \tag{4.8}$$

for each voice. Although in the undecimated case this remains equivalent to (4.7), in the decimated case, it implements a DWT corresponding to the hybrid family of wavelets

$$\psi_{i,n}^v \triangleq (\psi^v)_{i,n} = \frac{1}{\sqrt{2^i\gamma^v}}\,\psi\left(\frac{t}{2^i\gamma^v} - \frac{n}{\gamma^v}\right) \ . \tag{4.9}$$

Decimated voices are rarely implemented, but when they are, one invariably uses $\psi_{i,n}^v$ rather than $\psi_{iv,n}$.

Proceeding on the basis of (4.7) and (4.9), we retain the output grids $\Delta b = 1$ for undecimated wavelets and $\Delta b = 2^i$ for decimated wavelets, while incrementing a in (4.5) by $\Delta v = 1$. Note that a change of v by L is equivalent to an octave; i.e., to $\Delta i = 1$. Thus, $d(\ln a) \approx \Delta(i + v/L)\ln 2 = \ln 2/L$. Substituting these expressions into (4.1) yields

$$s(t) \approx Re\,\frac{2}{C_\psi}\frac{\ln 2}{L}\sum_{i,v,n} W_n^{iv}\,\frac{1}{2^i\gamma^v}\psi_n^{iv}(t) \ . \tag{4.10a}$$

for the undecimated wavelets, and

$$s(t) \approx Re\,\frac{2}{C_\psi}\frac{\ln 2}{L}\sum_{i,v,n} W_{i,n}^{v}\,\frac{1}{\gamma^v}\psi_{i,n}^{v}(t) \ . \tag{4.10b}$$

for decimated wavelets. The corresponding duals are

$$\widetilde{\psi_n^{iv}} \approx \frac{2\ln 2}{C_\psi L}\frac{1}{2^i\gamma^v}\psi_n^{iv} \tag{4.11a}$$

$$\widetilde{\psi_{i,n}^{v}} \approx \frac{2\ln 2}{C_\psi L}\frac{1}{\gamma^v}\psi_{i,n}^{v} \ . \tag{4.11b}$$

It should be emphasized that these expressions for the duals are mainly intended to serve as conceptual guidelines. For narrowband wavelets, the quality of the approximation is certainly in question.

The normalizations (4.7)–(4.9) have several advantages. The squares of all three types of wavelet coefficients represent power per Hz. This follows from the "Plancherel" formula (cf. Appendix D)

$$\begin{aligned} Energy \ = \ \int |s(t)|^2 dt \ &= \ \frac{2}{C_\psi}\int_0^\infty \int_{-\infty}^\infty \frac{da\,db}{a^2}\,|W_b^a|^2 \\ &\approx \ \frac{2}{C_\psi}\frac{\ln 2}{L}\sum_{i,v,n}\frac{1}{2^i\gamma^v}|W_n^{iv}|^2 \ . \end{aligned} \tag{4.12}$$

Equation (4.7), implies that the bandwidth of ψ_n^{iv} is proportional to $1/(2^i\gamma^v)$ so that the measure in the integral (4.12) is in units of $seconds \cdot Hz$. This, in turn, implies that the $|W_n^{iv}|^2$ is essentially power/Hz [2]. The same remains true of $W_{iv,n}$ and $W_{i,n}^v$ since they are simply nonuniform samples of the same density function; that is, of $W^{iv}(n)$. Furthermore, this normalization may be simply characterized as that which maintains the norms of the analyzing wavelets:

$$\|\psi_n^{iv}\| \ = \ \|\psi_{iv,n}\| \ = \ \|\psi_{i,n}^v\| \ = \ \|\psi\| \ . \tag{4.13}$$

A different density, perhaps more in the spirit of scaling functions, is power/scale where the units of scale are $\ln(a)$. This normalization, used for example in [8], results in analyzing wavelets of the form

$$\frac{1}{2^i\gamma^v}\,\psi\left(\frac{t-n}{2^i\gamma^v}\right) \ = \ \frac{1}{a}\psi\left(\frac{t-b}{a}\right) \ . \tag{4.14}$$

Another normalization, the symmetric one of [3] approximates self-dual wavelets; i.e., $\widetilde{\psi_{i,n}^v} \approx const \cdot \psi_{i,n}^v$ where the constant is independent of i and v. This is achieved by including the square root of the coefficient appearing in (4.11b) in the normalization of ψ_i^v. Thus, $\psi_{i,n}^v$ gets replaced by $\gamma^{-v/2}\psi_{i,n}^v$, that is, by $2^{-i/2}\gamma^{-v}\psi(2^{-i}\gamma^{-v}t - \gamma^{-v}n)$. However, this symmetric normalization, results in transforms which are not densities. Their squares are energy/cell where the cell size varies with scale and, hence, is difficult to interpret. As far as the composition $DWT^{-1} \circ DWT$ is concerned, the normalizing factor may be arbitrarily split between the wavelets and their duals. However, (a) different choices will

change the appearance/interpretation of the wavelet transform image, (b) each choice corresponds to a different left inverse,[8] and (c) the implementations/approximations of the various inverses may exhibit significantly different behavior.

B. *Single-integral inverse (Morlet formula)*

A second, less frequently used formula, is the so-called Morlet inversion formula ([8], Appendix D)

$$s(t) \;=\; Re\left\{\frac{2}{C_{1\psi}}\int_0^\infty \frac{da}{a^{3/2}}\,W_t^a\right\}\;, \tag{4.15}$$

where either ψ is analytic or $\widehat{\psi}(\omega)$ is real,

$$C_{1\psi} \;\triangleq\; \int_{-\infty}^{\infty}\frac{\overline{\widehat{\psi}(\omega)}}{|\omega|}\,d\omega\;, \tag{4.16}$$

and $W_t^a = W(a,t)$ defined in equation (1.3). For Morlet wavelets $\widehat{\psi(\omega)}$ is real, and, for practical purposes, $\psi(t)$ is analytic. The subscript of $C_{1\psi}$ is intended to reflect the L^1 dependence on $\widehat{\psi}$ in (4.16) as opposed to its modulus squared which appears in (1.1). The computational advantage of a single integration is enticing, and we shall find that the corresponding discrete formula is quite effective when applied to undecimated wavelets.

Discretizing, as in the previous subsection, we obtain

$$s(t) \;\approx\; Re\,\frac{2}{C_{1\psi}}\frac{\ln 2}{L}\sum_{i,v}\frac{1}{\sqrt{2^i\gamma^v}}\,W_t^{iv}\;. \tag{4.17}$$

The continuous time dependence of the coefficients W_t^{iv} in (4.17) prevents a direct interpretation as a dual expansion; however, if we discretize the output and define the vector $\boldsymbol{\delta}^n$ by $[\boldsymbol{\delta}^n]_m = \delta_{nm}$, then we may rewrite that expression as $\mathbf{s} \approx \sum_{ivn} W_n^{iv}\widetilde{\mathbf{x}_n^{iv}}$ where

$$\widetilde{\mathbf{x}_n^{iv}} \;=\; \frac{2}{C_{1\psi}}\frac{\ln 2}{L}\frac{\boldsymbol{\delta}^n}{\sqrt{2^i\gamma^v}}\;. \tag{4.18}$$

The formulae for the decimated wavelets are essentially the same since there is no integration over b. However, when we discretize the time by setting $\mathrm{w}_{iv,n} = W_{2^in}^{iv}$, we see that not all octaves are present (i.e, not all octaves have coefficients) at each integral time n. The lack of these values can have a crippling effect on the inversion approximation (cf. Section V).

We remark that both of the inversion formulae that we have presented are special cases of a more general family of inverses (cf. Appendix D)

$$s(t) \;=\; \frac{1}{C_{AB}}\int_{-\infty}^{\infty}\frac{da}{a^2}\int_{-\infty}^{\infty}db\;\left\langle s,(\psi^A)_b^a\right\rangle\overline{(\psi^B)_b^a(t)} \tag{4.19}$$

[8] That is, the duals are computed under different metrics, cf. Section III

where

$$C_{AB} \triangleq \int_{-\infty}^{\infty} \frac{\overline{\widehat{\psi^A}(\omega)}\,\widehat{\psi^B}(\omega)}{|\omega|} d\omega \ . \tag{4.20}$$

Equation (4.1) is derived by setting $\psi^A(t) = \psi^B(t) = \psi(t)$, while (4.15) follows from $\psi^B(t) = \delta(t)$. Additional manipulations and restrictions on ψ allow one to replace the integral over negative a by twice the real part.

C. *Relation to DWT*

Let us now relate some of the above approximations to the discrete wavelet transform. We examine the *undecimated* DWT of figure 2a invoking the approximation $\mathrm{w}_n^i \approx W_n^i$. It is clear that, if there are M stages, then $\mathbf{s}^M$ replaces the coefficients W_n^i for $i \geq M$. If we consider $\mathbf{s}^M$ as a discretized signal and take its wavelet transform, (4.12) with a single voice implies

$$\frac{1}{2^M} \|\mathrm{s}^M\|^2 \approx \frac{2\ln 2}{C_\psi} \sum_M^\infty \frac{1}{2^i} \|\mathbf{w}^i\|^2 \ , \tag{4.21}$$

where $\|\mathbf{w}^i\|^2 = \sum_n \|\mathrm{w}_n^i\|^2$. Substituting(4.21) back into (4.12) then yields

$$\|\mathbf{s}\|^2 \approx \|s(t)\|^2 \approx \frac{2\ln 2}{C_\psi} \sum_{i=0}^{M-1} \frac{1}{2^i} \|\mathbf{w}^i\|^2 + \frac{1}{2^M} \|\mathrm{s}^M\|^2 \ . \tag{4.22}$$

When its approximations hold, this equation implies a relationship between the normalizations of the filters $\boldsymbol{f}$ and $\boldsymbol{g}$. Consider the output of a one-stage ($M = 1$) filterbank where the discrete signal is an impulse function $\mathbf{s} = \boldsymbol{\delta}$. We have $\|\mathbf{s}\| = 1$, $\mathbf{w}^0 = \boldsymbol{g}$, and $\mathbf{s}^1 = \boldsymbol{f}$ giving

$$\frac{2\ln 2}{C_\psi} \|\boldsymbol{g}\|^2 + \frac{1}{2} \|\boldsymbol{f}\|^2 \approx 1 \ . \tag{4.23}$$

Multiple voices are easily implemented by making L copies of the filter bank, each with a different filter $\boldsymbol{g}^v$

$$g_n^v = \frac{1}{\sqrt{\gamma^v}} \psi\left(\frac{n}{\gamma^v}\right) \ . \tag{4.24}$$

Note that as long as (4.24) is a good piecewise approximation to ψ, we will also have $\|\boldsymbol{g}^v\| \approx \|\psi\|$, which we shall always assume to be one. The general expression (4.12) for the total energy, with voices, takes the form

$$\|\mathbf{s}\|^2 \approx \frac{2\ln 2}{C_\psi} \sum_{i=0}^{M-1} \frac{1}{2^i} \frac{1}{L} \sum_{v=0}^{L-1} \frac{1}{\gamma^v} \|\mathbf{w}^{iv}\|^2 + \frac{1}{2^M} \|\mathrm{s}^M\|^2 \ , \tag{4.25}$$

while (4.23) becomes

$$\frac{2\ln 2}{C_\psi} \frac{1}{L} \sum_v \frac{1}{\gamma^v} \|\boldsymbol{g}^v\|^2 + \frac{1}{2} \|f\|^2 \approx 1 \ . \tag{4.26}$$

It is not difficult to show that (Appendix A)

$$\sum_{v=0}^{L-1} \frac{1}{\gamma^v} = \frac{1}{2(1-2^{-1/L})} \approx \frac{L}{2\ln 2} , \tag{4.27}$$

so that (4.26) becomes

$$\frac{1}{C_\psi} + \frac{1}{2}\|\boldsymbol{f}\|^2 \approx 1 . \tag{4.28}$$

To be energy preserving, the wavelets must not be too redundant or too sparse. If they exactly fill the spectrum; that is, if $const \cdot \sum_v \gamma^{-v}|\boldsymbol{g}_x^v(\omega)|^2 + \frac{1}{2}|\boldsymbol{f}_x(\omega)|^2 = 1$, then the approximations are exact [9].

D. *Examples*

We examine the quality of the above approximations relative to our prototype non-orthogonal wavelet transform, namely, the DWT with $\boldsymbol{g}$ based on a Morlet wavelet and $\boldsymbol{f}$ an à trous filter (i.e., $f_{2n} = \delta_{n0}/\sqrt{2}$, [2]). The Morlet wavelet of L^2 norm one takes the form $\psi_M(t) = \beta^{1/2}\pi^{-1/4}e^{i\nu t}e^{-\beta^2 t^2/2}$. Its v^{th} voice, $\gamma^{-v/2}\psi_M(\gamma^{-v}t)$, has a relative bandwidth of β/γ^v. Requiring that these voices cover the upper half of the spectrum results in the following condition, which relates L and β (cf. Appendix A)

$$\beta \sum_{v=0}^{L-1} \frac{1}{\gamma^v} \geq \frac{\pi}{4\sqrt{2}} . \tag{4.29a}$$

or, from (4.27)

$$L \geq -\frac{\ln 2}{\ln(1-0.9\beta)} . \tag{4.29b}$$

We remark that the minimum number of voices satisfying (4.29) is approximated, conservatively, by $L = 1/\beta$. C_ψ is, of course, a function of β. It takes on the values 2.6, 2.26, and 2.12 for β equal to 0.5, 0.25, and 0.125 respectively. As β approaches 0, C_ψ approaches 2.0. That is, the set $\boldsymbol{g}^v$ acts as a perfect highpass filter (cf. ((4.28)). For L=1, equation (4.29b) is an equality for $\beta = 0.56$. That value of β implies that $C_\psi = 2.76$ which results in $2\ln 2/C_\psi = .502$. For L= 8, we get $\beta = 0.092$, $C_\psi = 2.09$, and, using $\|\boldsymbol{g}^v\| = 1$ along with (4.27), we find that the first term in (4.26) has the value 0.499.

Two typical interpolating filters $\boldsymbol{f}$ are the Lagrange à trous filters $(1/2,\ 1,\ 1/2)/\sqrt{2}$ and $(-1/16,\ 0,\ 9/16,\ 1,\ 9/16,\ 0,\ -1/16)/\sqrt{2}$ which have squared norms of 0.75 and 0.82 respectively. Ideally, we would like the lowpass filter $\boldsymbol{f}$ and the set of highpass filters $\boldsymbol{g}^v$ to split the energy spectrum into two equal parts [2]. In reality, $\boldsymbol{f}$ and $\boldsymbol{g}$ are not orthogonal so that some energy is bound to leak across scales. In fact, one-half of the above values are 0.375 and 0.41 respectively, so that $(1/2)\|\boldsymbol{f}\|^2$ equals 0.5 only very approximately. This can be interpreted as a need to compensate in the energy expression for the lack

of orthogonality between the lowpass and highpass filters. It would seem reasonable to correct this discrepancy by actually choosing C_ψ in (4.26) to satisfy

$$\frac{2\ln 2}{C_\psi}\frac{1}{L}\sum_v \frac{1}{\gamma^v} = 1 - \frac{1}{2}\|\boldsymbol{f}\|^2 \ , \tag{4.30}$$

where $\|\boldsymbol{g}^v\| = 1$.

As another interesting example, we examine the Haar wavelets. Appropriate DWT filters are $\boldsymbol{f} = (1,\ 1)/\sqrt{2}$ and $\boldsymbol{g} = (-1,\ 1)/\sqrt{2}$, resulting in exact wavelet coefficients (if $\mathbf{s}^0$ is in the appropriate subspace) for a continuous transformation with the mother wavelet

$$\psi_g(t) = \begin{cases} -1/\sqrt{2}, & \text{for } -1 \le t \le 0 \\ 1/\sqrt{2}, & \text{for } 0 \le t \le 1 \\ 0 & \text{otherwise} \end{cases} \ . \tag{4.31}$$

We have added the subscript g because the Haar wavelet $\psi(t)$ is more commonly taken to be $\psi_g(2t)/\sqrt{2}$. The difference springs from maintaining consistency with the relationship $g_n = \overline{\psi_g(-n)}$ of the generalized DWT, and is reflected by the fact that the usual orthonormal filter bank's first stage output is interpreted as scale 1 rather than scale 0 (see [2]). A nontrivial computation yields $C_{\psi_g} = 4\ln 2$. Consequently, the first coefficient in (4.23) is $(2\ln 2)/(4\ln 2) = 1/2$. Since the norms of $\boldsymbol{f}$ and $\boldsymbol{g}$ are 1, (4.23) holds exactly. This exact result is somewhat surprising inasmuch as C_ψ was computed from the continuous wavelet and the sums in the formulae were obtained by approximating an integral.

V. THE DISCRETE INVERSE

A major goal of this section is to develop and redefine previous concepts, such as energy and the inverse wavelet transform, entirely in discrete terms. We shall find this tantamount to a specification of filterbank implementations and a description of their properties. In keeping with this spirit, we reserve the term discrete inverse wavelet transform DWT^{-1} to mean precisely the family of transformations computed by the filter bank of figure 2b. The notation $\tilde{\boldsymbol{f}}$, $\tilde{\boldsymbol{g}}$ is intended to be suggestive, but these filters are not, even in a discrete sense, dual vectors. We also remark that the specific implementations considered are for a real signal $\mathbf{s}$. That is, we seek to recover the signal from the approximation $\mathbf{s} \approx Re\,\tilde{\mathbf{s}}$, that is, the real part of the DWT^{-1} (cf., equation (4.1)). A wide variety of approximate inverses, several of which are variations on the standard frame approximation (1.16), are obtained simply by varying these filters. We shall find that the DWT^{-1} can achieve better results than (1.16) with comparable or even less computation. (A price is paid, however, in the forward transformation since we require the undecimated transform.) Moreover, unlike (1.16), all such inverses are translation invariant. That is, the composition $DWT^{-1} \circ DWT$ commutes with translations.

A. *Filter Constraints*

Clearly, an attempt to treat banks of arbitrary filters would be much too general and unlikely to produce a very useful theory. In this subsection, we propose some minimal constraints on the forward and backward filters. At the very least, the DWT should be interpretable as a time-scale decomposition, should be numerically stable, and should have a stable inverse. For example, it is standard to require that $\boldsymbol{f}$, $\boldsymbol{g}$ be a lowpass-highpass filter pair, that $\boldsymbol{f}$ be real, and that $\sum_n f_n = \sqrt{2}$ before considering the forward filter bank a DWT [2]. An analysis of numerical behavior is beyond the scope of this work; however, we do present conditions for finite energy and boundedness of the DWT and DWT^{-1} as the number of stages M becomes infinite. These properties are important inasmuch as they reflect directly on the numerical stability of the algorithms themselves [4]. Even though one never actually computes an infinite number of octaves, the poor numerical behavior of unbounded transformations tends to persist for finite M.

Although an appropriate expression for the energy of the discrete nonorthogonal transform is somewhat arbitrary, we take one which is consistent with energy preservation in the biorthogonal case, and which mirrors the results of the previous section. First, we require the existence of $c_E > 0$ satisfying (cf. equation (4.26))

$$c_E \left(\frac{1}{L} \sum_v \frac{\|\boldsymbol{g}^v\|^2}{\gamma^v} \right) + \frac{1}{2}\|\boldsymbol{f}\|^2 = 1 \ . \tag{5.1}$$

We then define the energy by

$$\mathbf{E} \triangleq \sum_{i=0}^{M-1} \sum_{v=0}^{L-1} \frac{1}{2^i \gamma^v L} c_E \|\mathbf{w}^{iv}\|^2 + \frac{1}{2^M}\|\mathbf{s}^M\|^2 \ . \tag{5.2}$$

This is to be interpreted to mean that $(\sqrt{c_E}\mathbf{w}^{iv}, \mathbf{s}^M)$ is an energy density for the DWT and the total energy is given by applying the metric given by the $(ML+1)$-dimensional diagonal matrix with elements $\{2^{-i}\gamma^{-v}L^{-1}, 2^{-M}\}$. Although it may seem strange that the definition of $\mathbf{E}$ in equation (5.2) depends on the filters, the offending constant c_E is needed to balance the energy between $\boldsymbol{f}$ and the $\boldsymbol{g}^v$'s. Alternatively, we could have absorbed c_E into the filter $\boldsymbol{g}$ or used a different mother wavelet $\psi_{fg} \approx \sqrt{c_E}\psi$. [9] Suppose that $\boldsymbol{f}$ is a lowpass filter in the sense that $|\boldsymbol{f}_z(\omega)| < \sqrt{2}$ for $\omega \neq 0$ (recall that $\boldsymbol{f}_z(0) = \sqrt{2}$). Then, the last term, which represents the energy in the spectral interval $[0,\ 1/2^M]$, goes to zero as M goes to infinity (cf. Appendix B). Thus, the constant c_E represents a constant factor in the non-DC energy .

Perhaps the most significant aspect of the definition (5.2) is the fact that, for $M = \infty$, the discrete transform is bounded and has a bounded inverse if and only if there exist $A,\ B > 0$ such that

$$A\,\|\mathbf{s}\|^2 \ \leq\ \mathbf{E}(\mathbf{w}) \ \leq\ B\,\|\mathbf{s}\|^2 \ . \tag{5.3}$$

We point out that (5.3) is actually a discrete admissibility condition. The following is a sufficient condition for it to be satisfied [2]

$$0 \ <\ A \ \leq\ \frac{\frac{1}{2}\sum_v \frac{1}{L}\frac{c_E}{\gamma^v}|\boldsymbol{g}_z^v(\omega)|^2}{1-\frac{1}{2}|\boldsymbol{f}_z(\omega)|^2} \ \leq\ B \ <\ \infty \quad \textit{for all } \omega \ . \tag{5.4}$$

At $\omega = 0$, (5.4) is also a necessary condition (see Appendix B). Hence, we must have

$$\frac{1}{2}|\boldsymbol{f}_z(0)|^2 \leq 1 \ . \tag{5.5}$$

Note that, since $\boldsymbol{f}_z(0) = \sum_n f_n = \sqrt{2}$, condition (5.4) requires $\sum_n g_n^v = 0$ for all v, that is, that all the $\boldsymbol{g}^v$ be highpass filters. The DWT will be energy preserving (that is, $E = \|\mathbf{s}\|^2$) if and only if (5.4) holds with $A = B = 1$ [2].

Finiteness of the DWT^{-1} as $M \rightarrow \infty$ also imposes some constraints. The forward and inverse transforms include terms containing the filters $\boldsymbol{f}$ and $\widetilde{\boldsymbol{f}}$ iterated M times respectively. We cannot permit these terms to grow without bounds. More precisely, the output of the DWT^{-1} is given by (cf., figure 2b)

$$\widetilde{\mathbf{s}} \ =\ \sum_{i=0}^{M-1}\prod_{j=0}^{i-1}\left[(\mathbf{D}^j\widetilde{\boldsymbol{f}})*\right](\mathbf{D}^i\widetilde{\boldsymbol{g}})*\mathbf{w}^i \ +\ \prod_{j=0}^{M-1}\left[(\mathbf{D}^j\widetilde{\boldsymbol{f}})*\right]\mathbf{s}^M \ . \tag{5.6}$$

For $i = 0$, the first term on the right is understood to mean $\widetilde{\boldsymbol{g}}*\mathbf{w}^0$. Also, equivalent to the condition that $\psi(t)$ be real or analytic, we require that either both $\boldsymbol{g}$ and $\widetilde{\boldsymbol{g}}$ are real or one

[9] This would make some sense, since it makes the role of $\boldsymbol{f}$ more explicit in the relationship of the continuous and discrete transforms. Each filterbank has a "true" mother wavelet associated to it, which only approximates the original ψ. See [2], [10].

of them is analytic (that is has zero z-transform for $\omega < 0$). If the inverse is to be bounded in the metric of equation (5.2), then uniformly bounded inputs $\mathbf{w}^i$, $\mathbf{s}^M$ must produce uniformly bounded outputs. Taking z-transforms, we find this entails that $\int |\mathbf{s}_z^M(\omega)|^2/2^M$ uniformly bounded in M implies that $\int \prod_{j=0}^{M-1} |\widetilde{\boldsymbol{f}}_z(2^j\omega))|^2 \, |\mathbf{s}_z^M(\omega)|^2$ is uniformly bounded. This, in turn, implies

$$|\widetilde{\boldsymbol{f}}_z(0)| \leq \frac{1}{\sqrt{2}} \ . \tag{5.7}$$

Similarly, if the composition of the forward and inverse transforms is to be bounded for arbitrary M, then we must have

$$|\widetilde{\boldsymbol{f}}_z(0)\boldsymbol{f}_z(0)| \ \leq \ 1 \ . \tag{5.8}$$

Note that, since we require that $\boldsymbol{f}_z(0) = \sqrt{2}$, (5.8) implies (5.7). Details and conditions on the inverse filters similar to (5.4) may be found in Appendix B.

Of course, it would be desirable that the DWT^{-1} be an exact left inverse. As described in the introduction, this will be true if and only if equation (1.14) holds. For multiple voices and complex wavelets, this takes the form

$$Re \sum_v \widetilde{\boldsymbol{g}}^v * \boldsymbol{g}^v \ + \ \widetilde{\boldsymbol{f}} * \boldsymbol{f} \ = \ \boldsymbol{\delta} \ . \tag{5.9}$$

If $\boldsymbol{f}$ and $\boldsymbol{g}$ are filters corresponding to orthonormal wavelets, then (5.9) will hold for a single voice with $\widetilde{\boldsymbol{f}} = \boldsymbol{f}^\dagger$ and $\widetilde{\boldsymbol{g}} = \boldsymbol{g}^\dagger$. Unfortunately, in the case of Morlet wavelets, backward filters $\widetilde{\boldsymbol{g}}^v$ which satisfy (5.9) are generally much too long for most applications. In contrast, even in the nonorthogonal case, we shall find that the adjoint filters $\boldsymbol{f}^\dagger$ and $\boldsymbol{g}^\dagger$ provide useful approximations. Other backward filters of interest are $\widetilde{\boldsymbol{f}} = c\boldsymbol{\delta}$ and $\widetilde{\boldsymbol{g}} = c\boldsymbol{\delta}$. These filters, which are motivated by the continuous inverses (4.1) and (4.15) will prove extremely effective. The constraint (5.7) takes the form

$$\widetilde{\boldsymbol{f}} = c\,\boldsymbol{f}^\dagger \ \textit{implies} \ \ c \leq 1/2 \ , \tag{5.10}$$

and

$$\widetilde{\boldsymbol{f}} = c\,\boldsymbol{\delta} \ \textit{implies} \ \ c \leq 1/\sqrt{2} \ . \tag{5.11}$$

B. *Adjoint DWT*

We pause, briefly, to show that the filters $\widetilde{\boldsymbol{f}} = \boldsymbol{f}^\dagger$ and $\widetilde{\boldsymbol{g}} = \boldsymbol{g}^\dagger$ yield the adjoint DWT. Let $\mathbf{H}^i$ and $\mathbf{L}^M$ be the linear transformations

$$\mathbf{H}^i \triangleq \prod_{j=0}^{i-1} \left[(\mathbf{D}^j\widetilde{\boldsymbol{f}}) * \right] (\mathbf{D}^i\widetilde{\boldsymbol{g}}) * \quad \textit{and} \quad \mathbf{L}^M \triangleq \prod_{j=0}^{M-1} \left[(\mathbf{D}^j\widetilde{\boldsymbol{f}}) * \right] \ . \tag{5.12}$$

From figure 2a, the forward transform DWT_{fg} is given by $\mathbf{w}^i = \mathbf{H}^i\mathbf{s}$ and $\mathbf{s}^M = \mathbf{L}^M\mathbf{s}$. For the Euclidean metric we have

$$\begin{aligned} <\mathbf{w},\, DWT_{fg}\,\mathbf{s}> &= \sum_{i,n} \mathrm{w}_n^i\, \overline{[\mathbf{H}^i\mathbf{s}]_n} \;+\; \mathrm{w}_n^M\, \overline{[\mathbf{L}^M\mathbf{s}^M]_n} \\ &= \sum_{i,n} [\mathbf{H}^{i\dagger}\mathbf{w}^i]_n\, \overline{s_n} \;+\; [\mathbf{L}^{M\dagger}\mathbf{s}^M]_n\, \overline{s_n} \\ &= \sum_{i} <\mathbf{H}^{i\dagger}\mathbf{w}^i,\, \mathbf{s}> \;+\; <\mathbf{L}^{M\dagger}\mathbf{s}^M,\, \mathbf{s}> \\ &= <DWT^{-1}_{f^\dagger g^\dagger}\,\mathbf{w}\,,\, \mathbf{s}>\,, \end{aligned} \tag{5.13}$$

where the last line follows from (5.6) with $\widetilde{f} = f^\dagger$ and $\widetilde{g} = g^\dagger$. This implies that $DWT^{-1}_{f^\dagger g^\dagger}$ is identical to $(DWT_{fg})^\dagger$. Our algorithm actually uses $\widetilde{f} = f^\dagger/2$ which also satisfies (5.8). It is easy to see that this yields the adjoint under the energy metric (5.2).

C. *Implementations*

In addition to the baffling number of inverses available for consideration, one of the most confusing aspects of this subsection is a repeated shifting between decimated and undecimated wavelets. The gist of these machinations is that, although our wavelet transforms as well as the inverse filterbanks will always be undecimated, the interpretation of and distinctions between the various inverses are more properly made by an appeal to the decimated case. Much of the misery disappears if one keeps in mind that $[\mathbf{w}_i^v]_n = [\mathbf{w}^{iv}]_{2^i n}$; that is, the two types of wavelet transform are simply different samplings of the same function and that they coincide at their common points. We also remind the reader that when g is complex, s corresponds to the real part of $\widetilde{\mathrm{s}}$, that is, $Re\,\widetilde{\mathrm{s}}$. For notational simplicity, in this subsection, we present our derivations using only a single voice and replacing the constant $2\ln 2/C_\psi$ by c. The implementations of three inverses will be discussed: the double-integral type resembling (4.3a), the adjoint DWT, and a single-integral type corresponding to (4.17). The first two bear an intimate relationship to the frame approximation.

C.1. *Double-integral type*

We begin with $\widetilde{f} = \delta/\sqrt{2}$ and $\widetilde{g} = c\,g^\dagger$. Abbreviating the last term of (5.6) by DC, we have

$$\begin{aligned} [\widetilde{\mathrm{s}}]_0 &= c \sum_{i=0}^{M-1} \frac{1}{\sqrt{2^i}} \left[(\mathbf{D}^i g^\dagger) * \mathbf{w}^i\right]_0 \;+\; DC \\ &= c \sum_{i=0}^{M-1} \frac{1}{\sqrt{2^i}} \sum_n \overline{g}_n \mathrm{w}^i_{2^i n} \;+\; DC \\ &= c \sum_{i=0}^{M-1} \frac{1}{\sqrt{2^i}} \sum_n \mathrm{w}_{i,n} \overline{g}_n \;+\; DC \end{aligned}$$

$$= c \sum_{i=0}^{M-1} \sum_n \frac{1}{\sqrt{2^i}} w_{i,n} \psi(-n) + DC$$

$$= c \sum_{i=0}^{M-1} \sum_n w_{i,n} \psi_{i,n}(0) + DC \ . \qquad (5.14)$$

Except for the DC term, this coincides with the standard approximation (1.16) at time $t = 0$.

We wish to extend this formula to arbitrary times $t = m$. Let $\mathbf{w}^i(m) \triangleq \mathbf{w}^i(\mathbf{T}_{-m}\mathbf{s})$ and $\mathbf{w}_i(m) \triangleq \mathbf{w}_i(\mathbf{T}_{-m}\mathbf{s})$ be the wavelet transforms obtained by first translating the signal by m points (cf. (2.9)). The idea is that these transforms are computed at (i.e., centered about) time m. In this context, the standard approximation

$$s_m = s(m) \approx Re\, c \sum_{i=0}^{M-1} \sum_n w_{i,n} \psi_{i,n}(m) = Re\, c \sum_{i=0}^{M-1} \sum_n w_{i,n}(0) \psi_{i,n}(m) \qquad (5.15)$$

utilizes wavelet coefficients "computed" at time 0. For $m = 0$, equation (5.15) gives $s_0 \approx Re \sum w_{i,n}(0) \psi_{i,n}(0)$. Also, it is apparent from the form of (5.15) that for $m \neq 0$, the decimated wavelets $\psi_{i,n}(m)$ extrapolate s(t) from time $t = 0$ to time $t = m$.[10] Since $w_{i,n+2^M}(0) = w_{i,n}(2^{M-i})$, the extrapolation is never longer than $2^M - 1$. Alternatively, we could translate the signal by m, compute $w_{i,n}$ on the translated signal $\mathbf{T}_{-m}\mathbf{s}$ (which by definition yields $w_{i,n}(m)$), and evaluate the expansion at time 0. This yields

$$s_m = [\mathbf{T}_{-m}\mathbf{s}]_0 \approx Re\, c \sum_{i=0}^{M-1} \sum_n w_{i,n}(m) \psi_{i,n}(0) \ , \qquad (5.16)$$

thereby avoiding any extrapolation. Note that (5.15) and (5.16) represent two quite different approximations. This is because the decimated DWT is not translation invariant; i.e., $w_{i,n}(m) \neq w_{i,n+m}(0)$. In fact, we would expect (5.16) to be a better approximation since it does not extrapolate. (The tradeoff is that we must compute $\mathbf{w}_i(\cdot)$ at every point, which is equivalent to computing the undecimated DWT.)

On the other hand, the undecimated transform and its inverse are time invariant. This implies that $\widetilde{s}_m = [\widetilde{\mathbf{T}_{-m}\mathbf{s}}]_0$. Substituting this into (5.14) yields

$$\widetilde{s}_m = [\widetilde{\mathbf{T}_{-m}\mathbf{s}}]_0 = c \sum_{i=0}^{M-1} \sum_n w_{i,n}(m)\, \psi_{i,n}(0) + DC \ , \qquad (5.17)$$

[10] We use the word extrapolate to emphasize that the contribution of a single $w_{i,n}$ is extrapolated via $\psi_{i,n}$. On the other hand, since in a sense we are spanning the gap of 2^i points between $w_{i,n}$ and $w_{i,n+1}$, which in turn depend on the entire signal $\mathbf{s}$, we are interpolating. This, of course, is a much more stable operation than strict extrapolation.

which, except for the DC term, coincides with (5.16). In summary, we have considered two approximations to $s(m)$: (i) the decimated transform computed at time 0 and employed in the corresponding wavelet expansion to approximate the signal at time m (equation (5.15)), and (ii) the decimated transform computed at time m used in the wavelet expansion to approximate $s(m) = [\mathbf{T}_{-m}\mathbf{s}]_0$ at the same time as the computation (equation (5.16)). As the number of scales M goes to infinity, the latter formula becomes identical to (5.17), that is to the DWT^{-1} (i.e., undecimated inverse filter bank) with $\widetilde{\boldsymbol{f}} = \boldsymbol{\delta}/, /\sqrt{2}$, and $\widetilde{\boldsymbol{g}} = \boldsymbol{g}^\dagger$. In fact, (5.17) represents an improvement over (5.16) since the DC term replaces the energy lost in truncating the expansion at $i = M-1$.

C.2. *Adjoint*

We already know, from (5.13), that the DWT^{-1} with $\widetilde{\boldsymbol{f}} = \boldsymbol{f}^\dagger/2$ and $\widetilde{\boldsymbol{g}} = \boldsymbol{g}^\dagger$ is the adjoint to the DWT. It also has a simple interpretation in terms of the frame approximation but which is a bit difficult to demonstrate. It is an average of approximations of the form (5.15). More precisely, let $\boldsymbol{f}^\dagger * \mathbf{D}$ be the operator which acts on vectors $\mathbf{x}$ by $(\boldsymbol{f}^\dagger * \mathbf{D})\,\mathbf{x} = \boldsymbol{f}^\dagger * (\mathbf{D}\,\mathbf{x})$. As discussed in [2], when $\boldsymbol{f}$ is an à trous filter this operator is a dyadic interpolator. That is, $[\boldsymbol{f}^\dagger * (\mathbf{D}\boldsymbol{g}^\dagger)]_m \approx 2^{-1/2}\psi(m/2)$ so that

$$[(\boldsymbol{f}^\dagger * \mathbf{D})^i \boldsymbol{g}^\dagger]_m \approx \frac{1}{\sqrt{2^i}}\psi\left(\frac{m}{2^i}\right) . \tag{5.18}$$

Furthermore, it can be shown (Appendix E) that the DWT^{-1} with $\widetilde{\boldsymbol{f}} = \boldsymbol{f}^\dagger/2$ and $\widetilde{\boldsymbol{g}} = c\,\boldsymbol{g}^\dagger$ yields

$$\widetilde{s}_m = c \sum_{i=0}^{M-1} \sum_{r=0}^{2^i-1} [(\boldsymbol{f}^\dagger * \mathbf{D})^i\, (\boldsymbol{g}^\dagger * \mathbf{w}_i(r))]_{m-r} + DC . \tag{5.19}$$

Substituting (5.18) in (5.19), we have

$$\widetilde{s}_m \approx c \sum_{i=0}^{M-1} \frac{1}{2^i} \sum_n \sum_{r=0}^{2^i-1} \mathrm{w}_{i,n}(r)\, \psi_{i,n}(m-r) + DC \tag{5.20}$$

where we have used (E.7). One may rewrite this as $c \sum_{i,r,n} \mathrm{w}^i_{2^i n+r}\, 2^{-i}\, \psi^i_{2^i n+r}(m)$ reflecting the approximation $\widetilde{\psi^i_k} \approx c\,\psi^i_k$ of (4.4a). We may consider the set of $2^{-i}\psi_{i,n}(m-r) = 2^{-i}\psi^i_{2^i n+r}(m)$ as the $2^{-i}\widetilde{\psi^i_k}$ with $k = 2^i n + r$ of (4.11a). On the other hand, the decimated interpretation is somewhat more enlightening. The decimated transform at octave i is invariant under translations of 2^i; i.e., $\mathrm{w}_{i,n}(2^i) = \mathrm{w}_{i,n+1}(0)$. For each value of $r = 0, \ldots, 2^i - 1$, we can use (5.15) to estimate s_m by extrapolating from time r to time m, that is, $s_m \approx Re \sum_{i=0}^{M-1} \sum_n \mathrm{w}_{i,n}(r)\, \psi_{i,n}(m-r)$. Equation (5.20) is simply an average of these extrapolations. Since the longer the extrapolation, the less likely we are to have a good approximation, the quality of this result should lie somewhere in between that of (5.15) and (5.17). However, since the double-integral type (5.17) not only provides a better approximation, but also requires much less computation (a scalar multiplication for $\boldsymbol{\delta}/\sqrt{2}$

versus a convolution for the filter $f^\dagger/2$), there seems to be little reason to use the adjoint inverse.

C.3. *Single-integral type*

Finally, we examine $\widetilde{g} = c\delta$ with $\widetilde{f} = \delta/\sqrt{2}$. This results in an inverse analogous to the single integration approximation (4.17). More precisely, substituting $\mathbf{D}^j\widetilde{f} = \delta/\sqrt{2}$ and $\mathbf{D}^j\widetilde{g} = c\delta$ into (5.6), we have

$$\widetilde{s}_m = \sum_{i=0}^{M-1} \frac{c}{\sqrt{2^i}} \mathrm{w}_m^i + \frac{s_m^M}{\sqrt{2^M}} \quad . \tag{5.21}$$

Essentially the same formula holds for decimated wavelets; i.e., with w_m^i replaced by $\mathrm{w}_{i,m}$. However, in that case not all octaves are available at each time. More precisely, if we set $m = 2^Q r + 2^M n$ where $2^Q r < 2^M$ and $Q < M$ is the largest integer satisfying such an expression, we have

$$\widetilde{s}_m \approx \sum_{i=0}^{Q} \frac{c}{\sqrt{2^i}} \mathrm{w}_{i,m/2^i} + [f * \mathrm{s}_Q]_{m/2^Q} \quad . \tag{5.22}$$

If one omits the DC term, this formula will provide very poor results, since at those points for which Q is small, up to one-half the energy may be omitted. Since it is common practice to use only the wavelet coefficients $\mathbf{w}_i$, this may explain the reticence of many people to use the single integration approximation. In contrast, (5.21) yields excellent results, often better than (5.17) or (5.20) (cf. Section VI). Moreover, this $\widetilde{DWT}^{-1}$ does not increase the temporal support beyond that of the wavelet coefficients, a property which is extremely helpful for filtering in the wavelet domain. These features, coupled with a high computational efficiency, make this inverse our choice for most applications.

D. *Normalizing* $\widetilde{g}^v$

In Section IV, we related particular realizations of the DWT^{-1} to discrete approximations to the continuous inverse. This correspondence was determined up to the DC term and a constant, i.e., $\widetilde{\mathbf{s}} \approx c\,\mathbf{s}$. In theory, this gives us two constants to adjust; one multiplying the DC term and the other multipling the wavelets. The general question of how to pick these constants (or for that matter more general backward filters) is complex, application dependent, and beyond the scope of this study. Here, we restrict ourselves to just a few cases. First, to avoid a dependence on M, we determine the constants from the consideration of a generic single stage of $DWT^{-1} \circ DWT$. We shall remark on two possibilities, both involving approximations to (5.9). The most natural is to minimize the error in the least squares sense. That is,

$$\min_{c,c'} \| c\,Re \sum_v \widetilde{g}_U^v * g^v + c' \widetilde{f}_U * f - \delta \|^2 \tag{5.23}$$

where the form of the backward filters is given by one of the implementations in the last subsection and the subscript U indicates the renormalizations $\widetilde{\boldsymbol{g}} = c\widetilde{\boldsymbol{g}}_U$ and $\widetilde{\boldsymbol{f}} = c'\widetilde{\boldsymbol{f}}_U$. We observe that if the zeroth component of (5.9) holds exactly , then the substitution $\widetilde{\boldsymbol{g}}_U = (\boldsymbol{g}^v)^\dagger/\gamma^v$ and $\widetilde{\boldsymbol{f}}_U = \boldsymbol{f}^\dagger/2$ yields $c\sum_v Re\,[\gamma^{-v}(\boldsymbol{g}^v)^\dagger * \boldsymbol{g}^v]_0 + (c'/2)\,[\boldsymbol{f}^\dagger * \boldsymbol{f}]_0 = 1$. That is, $c\sum_v \gamma^{-v}\,|\boldsymbol{g}^v\|^2 + (c'/2)\|\boldsymbol{f}\|^2 = 1$. This is simply (4.26) with $c = (2\ln 2)/(C_\psi L)$ and $c' = 1$.

A second approach is to require that the energy of the reconstruction match that of the signal. To do this in a signal independent manner is not generally possible. As a compromise we apply this requirement to a specific signal, namely an impulse, which has a flat spectrum. Setting the energy of the impulse response of a single stage of the DWT^{-1} o DWT equal to one yields $\|c\,Re\,\sum_v \widetilde{\boldsymbol{g}}_U * \boldsymbol{g}^v \;+\; c'\widetilde{\boldsymbol{f}}_U * \boldsymbol{f}\|^2 = 1.0$. Note that, because of the cross-terms, this differs from preserving the energy of the wavelet transform (cf. equation (5.1)). Rather, it attempts to take into account the nonorthogonality of $\widetilde{\boldsymbol{f}} * \boldsymbol{f}$ and $\widetilde{\boldsymbol{g}} * \boldsymbol{g}$. Contrary to intuition, informal trials indicate that it is a better choice than (5.23); i.e., $\|Re\,\widetilde{\mathbf{s}} - \mathbf{s}\|^2$ is smaller. It cannot be better, of course, for the case in which $M = 0$ and the signal is impulsive, but it does seem comparable and provides an improvement for $M > 0$. Finally, we have found that taking $c' = 1$ seems to work as well or better than any other value, so we shall accept that simplification. With the constant c included in the $\widetilde{\boldsymbol{g}}^v$'s, this condition then becomes

$$\|\sum_v \widetilde{\boldsymbol{g}}^v * \boldsymbol{g}^v \;+\; \widetilde{\boldsymbol{f}} * \boldsymbol{f}\|^2 \;=\; 1 \;. \tag{5.24}$$

The author postulates that other choices will at best provide a marginal improvement and that if more accuracy is desired, it is much more efficient to iterate the suggested implementations by using Algorithm 3.1 than to look for other normalizations of $\widetilde{\boldsymbol{f}}$ and $\widetilde{\boldsymbol{g}}$. Another alternative, which works very well in practice and which will also be evaluated in Section VI, is to determine c from the continuous approximations (4.3) and (4.17) by which $\widetilde{\boldsymbol{g}} = (2\ln 2)/C_\psi)\,\boldsymbol{g}^\dagger$ and $\widetilde{\boldsymbol{g}} = (2\ln 2)/C_{1\psi})\,\boldsymbol{\delta}$ respectively.

Let us combine these remarks with the results of subsection V.C to summarize the various DWT^{-1}'s under consideration. We also shall take advantage of this opportunity to add voices to our formulation wherever they were previously omitted. There are two choices of $\widetilde{\boldsymbol{g}}^v$ under consideration. The double integral type is given by

$$\widetilde{\boldsymbol{g}}^v \;=\; \frac{c_2}{\gamma^v}\,(\boldsymbol{g}^v)^\dagger; \quad \widetilde{\boldsymbol{f}} = \boldsymbol{\delta}/\sqrt{2} \tag{5.25a}$$

with c_2 determined by

$$\|\,c_2\,Re\,\sum_{v=0}^{L-1} \frac{1}{\gamma^v}\,(\boldsymbol{g}^v)^\dagger * \boldsymbol{g}^v \;+\; \widetilde{\boldsymbol{f}} * \boldsymbol{f}\,\|^2 \;=\; 1 \;. \tag{5.25b}$$

Alternatively, by analogy to the continuous case, we may set

$$c_2 \;\approx\; \frac{2\ln 2}{L C_\psi} \;. \tag{5.25c}$$

The voice normalization γ^{-v} in (5.25a) comes from generalizing (5.14) along the lines of (4.10b).

The single integral type (cf. (4.18)) is given by

$$\widetilde{\boldsymbol{g}}^v \;=\; \frac{c_1}{\sqrt{\gamma^v}}\,\boldsymbol{\delta}; \quad \widetilde{\boldsymbol{f}} = \boldsymbol{\delta}/\sqrt{2} \tag{5.26a}$$

with c_1 determined by

$$\| c_1 \; Re \sum_{v=0}^{L-1} \frac{1}{\sqrt{\gamma^v}} \boldsymbol{g}^v \;+\; \widetilde{\boldsymbol{f}} * \boldsymbol{f} \|^2 \;=\; 1 \tag{5.26b}$$

or by analogy to the continuous case

$$c_1 \;\approx\; \frac{2 \ln 2}{L C_{1\psi}} \;. \tag{5.26c}$$

One might, quite justifiably, wonder about the absence of $1/2^i$ in (5.25) or (5.26) when comparing them with (4.11) or (4.18). In the case of (5.25), it is (4.11b) not (4.11a) which is relevant. More precisely, the reader is reminded that, although the input to the DWT^{-1} is the undecimated transform w_n^{iv}, its output (5.17) corresponds to a time-shifted decimated inverse; that is, to (4.11b) which has no $1/2^i$. The filter $\widetilde{\boldsymbol{f}} = \boldsymbol{\delta}/\sqrt{2}$ does supply a factor of $1/\sqrt{2^i}$. However, it is absorbed into the normalization of $\psi_{i,n}$ as detailed in equation (5.14). This contrasts with the adjoint DWT^{-1} where $\widetilde{\boldsymbol{f}} = \boldsymbol{f}^\dagger/2$ results in an additional factor of $1/2$ ($f_0/2 = 2^{-3/2}$ versus $2^{-1/2}$) which actually appears in (5.20) so that the adjoint DWT^{-1}'s output corresponds to (4.11a). Finally, in the DWT^{-1} specified by (5.26), $\widetilde{\boldsymbol{f}} = \boldsymbol{\delta}/\sqrt{2}$ is repeated i times producing a factor of $1/\sqrt{2^i}$ which appears in (5.21) and corresponds to (4.17). A simple way to normalize $\widetilde{\boldsymbol{f}}$ is to take equality in (5.7); that is, $\sum_n \widetilde{f}_n = 1/\sqrt{2}$.

E. Summary

The following table summarizes the DWT^{-1} implementations treated in this section.

Table 5.1 DWT^{-1}

DWT^{-1}	$\widetilde{\boldsymbol{f}}$	$\widetilde{\boldsymbol{g}}^v$	$\widetilde{\mathbf{s}}$	Interpretation
Adjoint (Ad)	$\frac{1}{2}\boldsymbol{f}^\dagger$	$\frac{c_2}{\gamma^v}(\boldsymbol{g}^v)^\dagger$	(5.20)	adjoint of (1.11)
Double Integral (DI)	$\frac{1}{\sqrt{2}}\boldsymbol{\delta}$	$\frac{c_2}{\gamma^v}(\boldsymbol{g}^v)^\dagger$	(5.17)	approx (4.3b) to (4.1)
Single Integral (SI)	$\frac{1}{\sqrt{2}}\boldsymbol{\delta}$	$\frac{c_1}{\sqrt{\gamma^v}}\boldsymbol{\delta}$	(5.21)	approx (4.17) to (4.15)

Remarks

(a) The DWT^{-1} is computed using undecimated wavelets $\mathbf{w}^i$ according to figure 2.

(b) The relationship between $\psi(t)$ in the referenced equations and the filters $\boldsymbol{g}^v$ is given by $g_n^v = \overline{\psi^v}(-n) = \gamma^{-v/2}\overline{\psi}(-n/\gamma^v)$.

(c) In cases Ad and DI, it is assumed that $\boldsymbol{g}$ is real or that it is analytic; i.e., $\boldsymbol{g}_z(\omega) \approx 0$ for $\omega < 0$.

(d) In case SI, it is assumed that $\boldsymbol{g}$ is analytic or that $\boldsymbol{g}^{v\dagger} = \boldsymbol{g}$ (i.e., $\boldsymbol{g}_z(\omega)$ is real). Note that neither condition holds for the Daubechies orthonormal wavelets.

(e) The definitions of the constants c_2 and c_1 are found in (5.25) and (5.26) respectively.

(f) The factors $1/2$ and c_2/γ^v appearing in the filters of the adjoint imply that it is the adjoint with respect to the energy metric. See equation (5.2).

(g) In the case of an à trous implementation of Morlet wavelets, $\boldsymbol{f} = \boldsymbol{f}^\dagger$ is real symmetric and $(\boldsymbol{g}^v)^\dagger = \boldsymbol{g}$ is complex Hermitian. In that case, the $\dagger$'s may be omitted in table 5.1.

(h) The equations cited under $\widetilde{\mathbf{s}}$ involve decimated wavelet coefficients even though $\widetilde{\mathbf{s}}$ is equal to the output of the undecimated inverse. See the introduction to subsection V.C.

(i) The abbreviations, which will also be used in Section VI, are Ad=Adjoint, DI=Double Integration, SI=Single Integration.

VI. COMPARATIVE PERFORMANCE OF INVERSES

In this section, we compare the three DWT^{-1} filter banks featured in table 5.1. To this we add the standard frame approximation (5.15). The task is considerably more complex than might at first appear. The performance of these algorithms is bound to be both wavelet (including bandwidth, number of octaves and number of voices) and signal dependent. In addition, there are variations on the algorithms which we would like to investigate, such as the choice of c_1 and c_2 or the inclusion of the DC term. Also, one may apply Algorithm 3.1 to these DWT^{-1}'s resulting in true left inverses. The quality of the particular DWT^{-1} then becomes a question of the speed of convergence of the iterations. One perfectly legitimate question, that of the relative behavior of these inverses after filtering in the wavelet domain, is beyond the scope of this paper.

In order to put some reasonable bounds on what will be an essentially empirical study, we restrict ourselves to Morlet wavelets of the form

$$\psi(t) = \beta^{1/2}\,\pi^{-1/4}\,e^{i\,3\pi t/4}e^{-\beta^2 t^2/2} \tag{6.1}$$

and consider only two signals, a discrete impulse and a sinusoid. They are the prototype examples of two major classes of signals, narrowband and broadband. The former outputs the transfer function of the linear system $DWT^{-1} \circ DWT$ which may then be compared to that of a true left inverse, in this case a delta function. Except to examine the single stage behavior, we shall fix the number of octaves at three, that is, i = 0, 1, 2. The frequency bands of these octaves are [0.25, 0.5], [0.25, 0.125], and [0.125, 0.0625]. The sinusoid which we shall use is $\sin(0.1\,t)$, sampled at $\Delta t = 1$. Consequently, its energy is concentrated in the last octave. Other sinusoids yield similar results; however, it should be mentioned that the placement of the sinusoid frequency relative to the centers of the voices $\boldsymbol{g}^v$ does make a difference. Also, to avoid the effects of the onset and termination of the input (which resemble impulses and thus are broadband), the sinusoidal signal is generated from 0 to T, but only data in the interval [T/4, 3T/4] are used for comparing the signal to the wavelet inverse.

An extremely important aspect of this study is the choice of error criterion. The most obvious is to take a function of the difference $\mathbf{s} - \widetilde{\mathbf{s}}$. Although this works quite well in the case of the impulse, problems occur for the sinusoid. The algorithms produce an accurate sinusoidal inverse, but they do not preserve the amplitude; that is, they reproduce the signal up to a multiplicative factor. For example, for a sinusoidal signal of unit norm and one typical $DWT^{-1} \circ DWT$, the root mean square error for the raw inverse was 0.125, but after the inverse was normalized to have unit norm, the error was only 0.007. Under the same circumstances, the rms errors for the impulse were 0.33 and 0.34 respectively. Consequently, in order get a measure of the quality of the inverse exclusive of the amplitude factor, we shall base our criteria on normalized signals.

$$\Delta_n \triangleq \left| \frac{s_n}{\|\mathbf{s}\|} - \frac{\widetilde{s}_n}{\|\widetilde{\mathbf{s}}\|} \right| . \tag{6.2}$$

Our error function shall be the root mean square error

$$\epsilon_{rms} = \left(\sum_n \Delta_n^2 \right)^{\frac{1}{2}} = \frac{\|\mathbf{s} - \widetilde{\mathbf{s}}'\|}{\|\mathbf{s}\|} , \tag{6.3}$$

where $\widetilde{\mathbf{s}}' = (\|\mathbf{s}\|/\|\widetilde{\mathbf{s}}\|)\widetilde{\mathbf{s}}$. Another possible choice, for example, would be the maximum absolute error $\epsilon_{max} = \max_n \Delta_n$. For convenience and without loss of generality, the signal will always be chosen such that $\|\mathbf{s}\| = 1$. By also displaying the output energy $\|\widetilde{\mathbf{s}}\|^2$, which for a true left inverse should be 1.0, we keep an eye on the amplitude mismatch. We emphasize, however, that the discrepancy in the norms $\|\widetilde{\mathbf{s}}\|$ and $\|\mathbf{s}\|$ is signal dependent and simply renormalizing the inverse does not solve the problem. Clearly, when the signal consists of a mixture of narrowband and broadband components, the amplitude distortion introduced by the DWT^{-1} is more than a simple multiplicative factor.

In order to dispel the visual vacuum, we begin, in figure 3, with plots of three typical inverses. All three reproduce the impulse, but with noticeable side lobes. The large dip at zero for the frame approximation (Fr) is due to the lack of a DC term. The only other obvious qualitative difference is the smaller support of the single integration (SI) formula. A great deal more may be said from an examination of table 6.1. We are immediately struck by the high quality of the inverses for narrowband signals. Perhaps this accounts for the success of the standard approximation in many applications. On the other hand, the behavior for an impulsive signal are often inadequate. This implies that iteration may well be necessary and consequently should be an important consideration in evaluating the various inverses. The four inverses appearing in table 6.1 are presented in approximate order of quality. The SI inverse has the smallest error and is by far the most efficient to implement. Although only a few parameter values are presented here, these inverses seem to exhibit a similar relative behavior over a large range of values of β and of L.

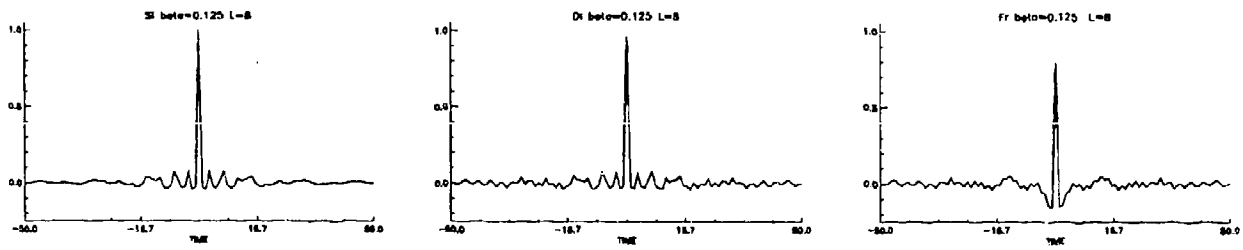

(a) (b) (c)

Figure 3. The transfer functions ($DWT \circ DWT^{-1}$) of three selected inverses. The signal is an impulse, and the forward transform is a Morlet wavelet with $\beta = 0.125$, four octaves, and 8 voices. The inverses shown are (a) single integration, SI; (b) double integration, DI, (c) and the frame approximation, Fr.

TABLE 6.1 Comparison of Four Inverses (3 octaves).

DWT^{-1}	β	L	impulse RMS	impulse ENERGY	sine RMS	sine ENERGY
SI	0.5	4	0.31	1.00	0.0024	1.19
	0.125	8	0.22	1.06	0.039	0.55
DI	0.5	4	0.34	0.88	0.0069	0.77
	0.125	8	0.26	0.99	0.044	0.49
Fr	0.5	4	0.50	0.65	0.0072	0.67
	0.125	8	0.39	0.87	0.050	0.60
Ad	0.5	4	0.32	0.96	0.0083	0.77
	0.125	8	0.54	0.78	0.067	0.31

Figure 4 illustrates the Neumann iterations (cf. Algorithm 3.1) for a DWT of type SI, and table 6.2 compares the results of such iterations for the four major types of inverses when the original signal is an impulse. Inasmuch as the energy rarely increased under $DWT \circ DWT^{-1}$ and always less than a factor of 2, μ was nominally set to 0.5. In the absence of other criteria, SI seems to be by far the best choice. The incredibly slow convergence for Fr is due to the lack of a DC term. (Optimizing μ made little difference. The iterations of Fr do not converge much faster for larger μ and diverge in the region of $\mu = 3$.) In fact, the same difficulties occur with the other inverses if the DC term is omitted. Without it, one must include a sufficient number of octaves to encompass all of the signal's energy whether or not a fine scale analysis of the lower frequency energy is of interest. For an impulse, whose energy covers the entire spectrum, an inverse without the DC term is particularly poor. Note that a DC term may be added to the Fr inverse by constructing the scale function $\phi(t)$ and including the term

$$\sum_n s_{M,n} \frac{1}{\sqrt{2^M}} \phi\left(\frac{m}{2^M} - n\right) \tag{6.4}$$

in equation (5.15). In view of the other inverses available, this does not seem to be worth the effort. It should be mentioned, however, that the frame expansion does provide a continuous interpolation of the signal (i.e., replace m by t), a property not shared by the DWT^{-1}. Finally, we remark that the difference between the expressions (5.25b) and (5.25c) for c_2 or between (5.26b) and (5.26c) for c_1 seems to be insignificant.

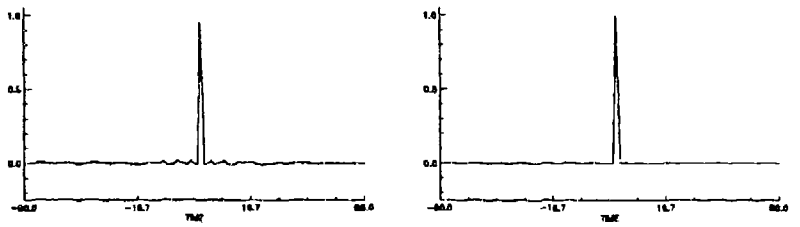

(a) (b)

Figure 4. The result of performing Neumann iterations on the inverse SI after (a) 5 iterations and (b) 10 iterations. The forward transform had $\beta = 0.125$ and $L = 8$; the iteration factor was $\mu = 0.5$.

TABLE 6.2 RMS errors of iterated DWT^{-1} with Morlet wavelets and implulsive signal; $\beta = 0.5$, 3 octaves, $L = 4$, $\mu = 0.5$.

DWT^{-1}	NUMBER OF ITERATIONS					
	1	5	10	25	50	100
SI	0.264	0.120	0.048	0.0038	0.000067	$2.9\ 10^{-7}$
DI	0.308	0.190	0.115	0.033	0.0050	0.00016
Fr	0.461	0.371	0.322	0.284	0.273	0.264
Ad	0.283	0.162	0.091	0.020	0.0021	0.00012

The number of voices, which is really a parameter of the forward transform, is particularly relevant to the quality of the inverse. The optimal number of voices (for a given β) tends to be that given by equation (4.29) with equality, that is, approximately $1/\beta$. Too few voices greatly degrades the results. Without iteration, additional voices make little difference. However, a degradation in the speed of convergence of the Neumann iterations does seem to take place with additional voices. For example, let $\beta = 0.25$, for which the suggested number of voices is $L = 3$. Then, the mse errors of SI at iteration 10 for $L = 1,\ 2,\ 3,\ 8$ are, respectively, 0.25, 0.018, 0.0032, and 0.028. This phenomenon is somewhat surprising inasmuch as adding voices tends to make a tighter frame [3], [4]. However, ultimately, convergence hinges on the specific eigenvalues of the functional iteration, which, in turn, depend on the filter $\boldsymbol{f}$ and on μ as well as the number of voices. The value used, $\mu = 0.5$, is well below the point of instability, which for the above range of parameters occurs between $\mu = 1.0$ and $\mu = 3.0$. The best convergence seems to occur near instability (although there is a short interval just before that point where it slows down). Further study would be needed to fully explain the situation. Note that the minimal values satisfying (4.29) for $\beta = 0.5$ and $\beta = 0.125$ are $L = 1$ and $L = 6$ respectively. However, since for visual presentation it is a good idea to use at least four voices, and since it is convenient to pick $L \approx 1/\beta$, we have used $L = 4$ and 8 in the above presentation.

VII. CONCLUSION

The standard inversion procedure for discrete nonorthogonal transforms is a finite expansion in terms of the analyzing wavelet. While this so-called wavelet series or frame approximation works quite well for many signals, it fails to achieve good accuracy or requires an excessive number of scales for others. To remedy the situation, we have proposed an inverse filter bank DWT^{-1} as a prototype inverse discrete wavelet transform. It provides a unifying framework under which the various (approximate) left inverses are obtained by varying the filters. For example, it was shown that the adjoint transformation of the undecimated discrete wavelet transform is computed by using the adjoints of the filters from the forward transform. More generally, within this context, we have examined the properties and interrelationships of dual wavelets, metrics, pseudo-inverses, and discretizations of continuous inverses. In particular, we have found that the absence of decimation results in dual wavelets that are time invariant, and that the standard frame approximation may be interpreted as an interpolation of a DWT^{-1}. Finally, in addition to the adjoint, we proposed two other discrete left inverses, which use filters based on continuous integral formulae.

Two major differences stand out between the standard frame approximation and the inverses discussed in this paper. They are the use of the undecimated wavelet transform as input to the DWT^{-1} and the inclusion of a DC (low-frequency) term which is lacking in the frame approximation. Avoiding decimation does provide redundancy and, hence, a potentially better approximation. However, our preference for not decimating actually stems from the forward transform. A desire to achieve finer output resolution coupled with time invariance makes the undecimated DWT the natural setting for nonorthogonal wavelets. Given this situation, it makes sense to use an inverse that exploits all the numeric information available. The lack of a DC term in the frame approximation is a more serious issue. It leads to poor accuracy in the case of broadband signals and even implies that the composition of the forward and inverse transforms is singular so that iteration need not converge to a true left inverse.

The best among the inverses studied seems to be the single-integral inverse. This inverse is equivalent to simply summing the weighted wavelet coefficients across scale. It is by far the most efficient computationally, is generally the most accurate, converges much more rapidly than others under iteration, and does not increase the support of the DWT. The latter property is quite useful, inasmuch as it implies that filtering in the wavelet domain is a quasi-local operation in time. That is, the value of the DWT^{-1} at a given time only depends on the wavelet coefficients at that time.[11] A potential drawback is that the single-integral inverse does not represent an orthogonal projection under the energy metric. However, to date the author has been unable distinguish any negative impact.

[11] We use the qualifier quasi because this does not remain true under iteration. That is, the corresponding exact left inverse is not a local operator.

VIII. REFERENCES

[1] Combes, J. M., A. Grossmann, and P. Tchamitchian, Eds., *Wavelets: Time-Frequency Methods and Phase Space*, Berlin: Springer, IPTI, 1989.

[2] Shensa, M. J., "The Discrete Wavelet Transform: Wedding the À Trous and Mallat Algorithms," *IEEE Trans. Signal Processing*, October 1992, pp. 2464–2482.

[3] Daubechies, I., *Ten Lectures on Wavelets*, SIAM, Philadelphia, 1992.

[4] Daubechies, I., "The Wavelet Transform, Time-frequency Localization and Signal Analysis," *IEEE Trans. Inf. Theory*, September 1990, pp. 961-1005.

[5] Grossmann, A., R. Kronland-Martinet, J. Morlet, "Reading and Understanding Continuous Wavelet Transforms," in *Wavelets: Time-Frequency Methods and Phase Space*, Berlin: Springer, IPTI, 1989, pp. 1-20.

[6] Shensa, M. J., "Inverting Narrowband Wavelets," *Proc. of* 14^{th} *GRETSI*, Juan-les-pins, France, September 1993.

[7] Benedetto, J. J. and A. Teolis, "An Auditory Motivated Time-scale Signal Representation," *Proc. IEEE-SP Intl. Symp. on Time-frequency and Time-scale Analysis,* October 1992.

[8] Delprat, N., P. Guillemain, R. Kronland, P. Tchamitchian, B. Torresani, "Asymptotic Wavelet and Gabor Analysis: Extraction of Instantaneous Frequencies,"*IEEE Trans. Inf. Theory*, March 1992, pp. 644–664.

[9] Mallat, S. and W. L. Hwang, "Singularity Detection and Processing with Wavelets," *IEEE Trans. Inf. Theory*, March 1992, pp.617-643.

[10] Rioul, O. and P. Duhamel, "Fast Algorithms for Discrete and Continuous Wavelet Transforms," *IEEE Trans. Inf. Theory*, March 1992, pp. 569-686.

APPENDIX A. MORLET WAVELETS

The generating Morlet wavelet (of L^2 norm one) takes the form

$$\psi(t) \;=\; \frac{\beta^{1/2}}{\pi^{1/4}}\, e^{i\nu t}\, e^{-\beta^2 t^2/2} \quad . \tag{A.1}$$

There are two parameters, ν and β; however, in general only the ratio β/ν is significant since the family

$$\psi^a(t) \;=\; \frac{1}{\sqrt{a}}\,\frac{\beta^{1/2}}{\pi^{1/4}}\, e^{i\nu t/a}\, e^{-\beta^2 (t/a)^2/2} \quad , \tag{A.2}$$

obtained by scaling only depends on β/ν. The Fourier transform of $\psi(t)$ is

$$\widehat{\psi}(\omega) \;=\; \pi^{1/4}\,\sqrt{2/\beta}\, e^{-(\omega-\nu)^2/2\beta^2} \quad , \tag{A.3}$$

and the energy normalization constants C_ψ and $C_{1\psi}$ of equations (1.1) and (4.16) are given by

$$\begin{aligned} C_\psi \;&\triangleq\; \int_{-\infty}^{\infty} \frac{|\widehat{\psi}(\omega)|^2}{|\omega|}\, d\omega \\ &=\; \sqrt{\pi}\,\frac{2}{\beta} \int_{-\infty}^{\infty} \frac{e^{(\omega-\nu)^2/\beta^2}}{|\omega|}\, d\omega \end{aligned} \tag{A.4}$$

and

$$\begin{aligned} C_{1\psi} \;&\triangleq\; \int_{-\infty}^{\infty} \frac{\overline{\widehat{\psi}(\omega)}}{|\omega|}\, d\omega \\ &=\; \pi^{1/4}\,\sqrt{\frac{2}{\beta}} \int_{-\infty}^{\infty} \frac{e^{(\omega-\nu)^2/2\beta^2}}{|\omega|}\, d\omega \quad . \end{aligned} \tag{A.5}$$

We define the half-bandwidth, $\Delta\omega$, and the half-duration, Δt, to be the point at which $|\widehat{\psi}|$ and $|\psi|$ fall to $1/e$ of their peak value; i.e.,

$$\Delta\omega \;=\; \sqrt{2}\,\beta \tag{A.6a}$$

$$\Delta t \;=\; \sqrt{2}\,/\,\beta \quad . \tag{A.6b}$$

The area occupied in phase space is thus

$$(2\,\Delta\omega)\,(2\,\Delta t) \;=\; 8.0 \;\approx\; 2\pi \quad . \tag{A.7}$$

Note that the ratio

$$\frac{\Delta\omega}{\Delta t} \;=\; \beta^2 \tag{A.8}$$

reflects the shape of the region. Smaller β increases frequency resolution while decreasing time resolution. Since (A.8) depends on β^2, the shape is fairly sensitive to β. At octave i relations (A.6) become $\Delta\omega = \sqrt{2}\,\beta\,/\,2^i$ and $\Delta t = 2^i\,\sqrt{2}\,/\,\beta$. Although the product of these two remains the same, their ratio is $\Delta\omega\,/\,\Delta t \;=\; \beta^2\,/\,2^{2i}$. Thus, (A.8) is a rather unsatisfying description of β. A more invariant and intuitively useful description of β is the relative frequency resolution. Since, the center frequency of ψ is $\nu\,/\,2^i$, the ratio of the bandwidth to the central frequency is $(2\sqrt{2}\,\beta\,/\,2^i)\;/\;(\nu\,/\,2^i) = 2\sqrt{2}\,\beta\,/\,\nu$, which is independent of i.

Discrete Case

For convenience, we set the sample rate to be 1. Thus, the highpass filter $\boldsymbol{g}$ is determined by the samples $\psi(n)$. Nyquist, the highest frequency representable, is $\omega = \pi$. Hence, in order to avoid aliasing we must pick

$$\nu \;\leq\; \pi - \sqrt{2}\,\beta \;. \tag{A.9}$$

For $\beta = 0.5$, the maximum value of ν is about $3\pi/4$. If ν is larger, the energy will alias, and the continuous function corresponding to $\boldsymbol{g}$ will not be the Morlet wavelet ψ. That is, the DWT will be the wavelet transform with respect to the aliased function. Also, in order that ψ be admissible, the spectrum must be essentially 0 for $\omega < 0$, which holds sufficiently closely if [2] - [5]

$$\beta \;\leq\; \frac{\nu}{2\,\pi} \;. \tag{A.10}$$

To achieve this, we take $\beta \leq 0.5$ and $\nu = \pi - 0.707$.

The bandwidth of the upper half of the spectrum is $\pi/2$. In order that the transform retain all the signal energy, and hence invert in a numerically stable fashion, the highpass filters must cover the spectrum from $\pi/2$ to π. That is, we must have enought voices to do this. If $\gamma = 2^{1/L}$ where L is the number of voices, then voice v has bandwidth $2\,\sqrt{2}\,\beta\,/\,\gamma^v$. Thus, the total bandwidth covered is

$$\begin{aligned} TBW \;&\approx\; 2\sqrt{2}\,\beta\,\left(1 + \frac{1}{\gamma} + \frac{1}{\gamma^2} \cdots \frac{1}{\gamma^{L-1}}\right) \\ &=\; \sqrt{2}\,\beta\,\frac{1}{1 - 2^{-1/L}} \;. \end{aligned} \tag{A.11}$$

Also,

$$\lim_{L\to\infty} \frac{1/L}{1 - 2^{-1/L}} \;=\; \frac{1}{\ln 2} \;. \tag{A.12}$$

Hence,

$$TBW \;\approx\; \sqrt{2}\,\beta\,\frac{L}{\ln 2} \;\approx\; 2\,L\,\beta \;. \tag{A.13}$$

To cover the spectrum, we must have $2\,L\,\beta \geq \pi/2$; i.e.,

$$L \;\geq\; \frac{0.79}{\beta} \;\approx\; \frac{1}{\beta}\;, \tag{A.14}$$

which is generally valid for $\beta \leq 0.25$. A more precise formula is obtained by setting (A.11) greater than $\pi/2$. That is, $\beta \geq (\pi\,/\,2\sqrt{2})\,(\,1-2^{-1/L}\,)$ which yields,

$$L \;\geq\; -\frac{\ln 2}{\ln(1-0.9\beta)}\;. \tag{A.15}$$

APPENDIX B. CONDITIONS FOR BOUNDED TRANSFORMS

We derive several conditions for uniform boundedness (i.e., as $M \to \infty$) of the DWT, the DWT^{-1}, and their composition. We begin with necessary conditions expressed as constraints on the filters at $\omega = 0$, and finish with a set of sufficient conditions (analogous to (5.4)) for boundedness of the composition. For notational clarity, we restrict the treatment to a single voice.

From figure 2,

$$\mathbf{w}^i = (\mathbf{D}^i \boldsymbol{g}) * \prod_{j=i-1}^{0} [(\mathbf{D}^j \boldsymbol{f}) *] \, \mathbf{s} \qquad (B.1a)$$

$$\mathbf{s}^{i+1} = \prod_{j=i}^{0} [(\mathbf{D}^j \boldsymbol{f}) *] \, \mathbf{s} \ , \qquad (B.1b)$$

with the obvious interpretation for $i = 0$ in (B.1a). Using (2.14), we obtain the z-transforms of (B.1) and (5.6)

$$\mathbf{w}_z^i(\omega) = \prod_{j=0}^{i-1} [\boldsymbol{f}_z(2^j\omega)] \, \boldsymbol{g}_z(2^i\omega) \, \mathbf{s}_z(\omega) \qquad (B.2a)$$

$$\mathbf{s}_z^M(\omega) = \prod_{j=0}^{M-1} \boldsymbol{f}_z(2^j\omega) \, \mathbf{s}_z(\omega) \qquad (B.2b)$$

$$\widetilde{\mathbf{s}}_z(\omega) = \sum_{i=0}^{M-1} \prod_{j=0}^{i-1} \widetilde{\boldsymbol{f}}_z(2^j\omega) \, \widetilde{\boldsymbol{g}}_z(2^i\omega) \, \mathbf{w}_z^i(\omega) + \prod_{j=0}^{M-1} \widetilde{\boldsymbol{f}}_z(2^j\omega) \, \mathbf{s}_z^M(\omega) \ . \qquad (B.3)$$

Composing (B.2) and B.3), we have

$$\widetilde{\mathbf{s}}_z(\omega) = \Bigg[\sum_{i=0}^{M-1} \prod_{j=0}^{i-1} \widetilde{\boldsymbol{f}}_z(2^j\omega) \prod_{j=0}^{i-1} \boldsymbol{f}_z(2^j\omega) \, \widetilde{\boldsymbol{g}}_z(2^i\omega) \, \boldsymbol{g}_z(2^i\omega) + \prod_{j=0}^{M-1} \widetilde{\boldsymbol{f}}_z(2^j\omega) \prod_{j=0}^{M-1} \boldsymbol{f}_z(2^j\omega) \Bigg] \mathbf{s}_z(\omega) \ . \qquad (B.4)$$

The metric induced by (5.2) is

$$\|(\mathbf{w}^i, \mathbf{s}^M)\|^2 = \sum_{i=0}^{M-1} \frac{c_E}{2^i} \|\mathbf{w}^i\|^2 + \frac{1}{2^M} \|\mathbf{s}^M\|^2 \ . \qquad (B.5)$$

It follows from (B.2) and (B.3) that (5.5) and (5.7) are necessary conditions for the DWT and DWT^{-1} to be bounded with respect to this metric. Also, from (B.4), equation (5.8)

is a necessary condition for their composition to be bounded. We demonstrate (5.5): If the DWT is bounded (as $M \to \infty$) there must exist $B > 0$) such that for all M and s

$$\frac{1}{2^M} \int |\mathbf{s}_z^M(\omega)|^2 \, d\omega \;\leq\; B \int |\mathbf{s}_z(\omega)|^2 \, d\omega \;=\; B \, \|\mathbf{s}\|^2 \;. \qquad (B.6)$$

Suppose that $|\boldsymbol{f}_z(0)| = \sqrt{2}(1+\beta) > \sqrt{2}$. Then, there exists an $\epsilon > 0$ such that $|\boldsymbol{f}_z(\omega)| \geq \sqrt{2}(1+\alpha) > \sqrt{2}$ for $|\omega| \leq \epsilon$. Take s such that $\mathbf{s}_z(\omega) = 0$ *for* $|\omega| > \epsilon/2^M$. Then $|\boldsymbol{f}_z(2^i\omega)|^2 \geq 2(1+\alpha)^2$ for $i \leq M$ and $|\omega| \leq \epsilon/2^M$ so that (B.2b) implies that

$$\begin{aligned} \frac{1}{2^M} \int |\mathbf{s}_z^M(\omega)|^2 \;&\geq\; \frac{1}{2^M} \, 2^M \, (1+\alpha)^{2M} \int_{|\omega| \leq \epsilon/2^M} |\mathbf{s}_z(\omega)|^2 \\ &=\; (1+\alpha)^{2M} \, \|\mathbf{s}_z\|^2 \;, \end{aligned} \qquad (B.7)$$

which contradicts (B.6). Thus, for boundedness, we must have $|\boldsymbol{f}_z(0)| \leq \sqrt{2}$. The other proofs utilize $\boldsymbol{g}_z(0) = \widetilde{\boldsymbol{g}}_z(0) = 0$.

We consider the composition $DWT^{-1} \circ DWT$ in more detail. From figure 2a, we have

$$\widetilde{\mathbf{s}}^i \;=\; (\mathbf{D}^i \widetilde{\boldsymbol{f}}) \widetilde{\mathbf{s}}^{i+1} \;+\; (\mathbf{D}^i \widetilde{\boldsymbol{g}}) \mathbf{w}^i \;. \qquad (B.8)$$

Taking the z-transform and combining it with that of figure 2b yields

$$\begin{aligned} \widetilde{\mathbf{s}}_z^i(\omega) \;&=\; \widetilde{\boldsymbol{f}}_z(2^i\omega) \widetilde{\mathbf{s}}_z^{i+1}(\omega) \;+\; \widetilde{\boldsymbol{g}}_z(2^i\omega) \, \mathbf{w}_z^i(\omega) \\ &=\; \widetilde{\boldsymbol{f}}_z(2^i\omega) \widetilde{\mathbf{s}}_z^{i+1}(\omega) \;+\; \widetilde{\boldsymbol{g}}_z(2^i\omega) \, \boldsymbol{g}_z(2^i\omega) \, \mathbf{s}_z^i(\omega) \;. \end{aligned} \qquad (B.9)$$

Lemma Suppose that

$$|\widetilde{\boldsymbol{f}}_z(\omega) \, \boldsymbol{f}_z(\omega)| \;+\; C^{-1} \, |\widetilde{\boldsymbol{g}}_z(\omega) \, \boldsymbol{g}_z(\omega)| \;\leq\; 1 \;\; for \, all \, \omega \qquad (B.10)$$

where $C \geq 1$. Then,

$$|\widetilde{\mathbf{s}}_z^i(\omega)| \;\leq\; C \, |\mathbf{s}_z^i(\omega)| \;. \qquad (B.11)$$

Proof For $i = M$, we have $\widetilde{\mathbf{s}}_z^M(\omega) = \mathbf{s}_z^M(\omega)$. Assume the lemma is true for i and prove it for $i-1$.

$$\begin{aligned} |\widetilde{\mathbf{s}}_z^{i-1}(\omega)| \;&\leq\; |\widetilde{\boldsymbol{f}}_z(2^{i-1}\omega) \widetilde{\mathbf{s}}_z^i(\omega)| \;+\; C^{-1} \, |\widetilde{\boldsymbol{g}}_z(2^{i-1}\omega) \, \boldsymbol{g}_z(2^{i-1}\omega) \, C \, \mathbf{s}_z^{i-1}| \\ &\leq\; |\widetilde{\boldsymbol{f}}_z(2^{i-1}\omega) \, C \, \mathbf{s}_z^i(\omega)| \;+\; C^{-1} \, |\widetilde{\boldsymbol{g}}_z(2^{i-1}\omega) \, \boldsymbol{g}_z(2^{i-1}\omega) \, C \, \mathbf{s}_z^{i-1}| \\ &=\; |\widetilde{\boldsymbol{f}}_z(2^{i-1}\omega) \, \boldsymbol{f}_z(2^{i-1}\omega) \, C \, \mathbf{s}_z^{i-1}(\omega)| \;+\; C^{-1} \, |\widetilde{\boldsymbol{g}}_z(2^{i-1}\omega) \, \boldsymbol{g}_z(2^{i-1}\omega) \, C \, \mathbf{s}_z^{i-1}| \\ &\leq\; C \, |\mathbf{s}_z^{i-1}(\omega)| \;. \end{aligned} \qquad (B.12)$$

A $C \geq 1$ satisfying (B.10) exists provided $|\widetilde{\boldsymbol{f}}_z(\omega) \boldsymbol{f}_z(\omega)| \leq 1$ and

$$\frac{|\widetilde{\boldsymbol{g}}_z(\omega) \, \boldsymbol{g}_z(\omega)|}{1 - |\widetilde{\boldsymbol{f}}_z(\omega) \, \boldsymbol{f}_z(\omega)|} \;\leq\; C \;<\; \infty \;\; for \, all \, \omega \;. \qquad (B.13)$$

(B.11) implies that $\|\widetilde{\mathbf{s}}\|^2 \leq C^2 \, \|\mathbf{s}\|^2$. If $\boldsymbol{g}$ is complex then, a forteriori, $\|Re \, \widetilde{\mathbf{s}}\|^2 \leq C^2 \, \|\mathbf{s}\|^2$. Thus, (B.13) is a sufficient condition for $DWT^{-1} \circ DWT$ to be a bounded transformation.

APPENDIX C. NOTES ON DUALS

The k^{th} column of a matrix represents the image under the transformation of the k^{th} basis vector in the domain. Thus, if $\mathbf{A}$ is a matrix representing the forward DWT, its k^{th} column $\mathrm{w}_{i,n} = [\mathbf{As}]_{\cdot,k}$ is the image of $[\mathrm{s}]_n = \delta_{kn}$. But, $\mathrm{w}_{i,n} \approx \sum_m s_m \psi_{i,n}(m) = \psi_{i,n}(k)$. Thus, the rows of $\mathbf{A}$ correspond to the basis vectors $\boldsymbol{\psi}_{i,n}(\cdot)$. Under this correspondence, we have

$$[(\mathbf{A}^\dagger\mathbf{A})^{-1}\mathbf{A}^\dagger]_{k;(i,n)} \approx \sum_m (\mathbf{A}^\dagger\mathbf{A})^{-1}_{k,m}\psi_{i,n}(m) \approx \widetilde{\psi_{i,n}}(k) \ .$$

In other words, the discrete pseudo-inverse $(\mathbf{A}^\dagger\mathbf{A})\mathbf{A}^\dagger\mathrm{w}$ may be interpreted as an expansion in terms of dual vectors where the duals $\widetilde{\boldsymbol{\psi}_{i,n}}(\cdot)$ are given by $(\mathbf{A}^\dagger\mathbf{A})^{-1}\boldsymbol{\psi}_{i,n}(\cdot)$ and $\boldsymbol{\psi}_{i,n}(\cdot)$ are the columns of $\mathbf{A}^\dagger$.

APPENDIX D. PLANCHEREL RELATIONS AND CONTINUOUS INVERSION FORMULAE

Let $\psi^1(t)$ and $\psi^2(t)$ be two admissible wavelet functions and $s^1(t)$ and $s^2(t)$ two signals in L^2. Then the inner product of the corresponding wavelet transforms, with respect to the measure $da\,db\,/a^2$, is equal to the inner product of the two signals up to a constant dependent on ψ^1 and ψ^2. That is [3],

$$\int_{-\infty}^{\infty} \frac{da}{a^2} \int_{-\infty}^{\infty} db \; <s^1,\, {\psi^1}_b^a><{\psi^2}_b^a,\, s^2> \;=\; C_{\psi^1\psi^2} <s^1,\, s^2> \;, \qquad (D.1)$$

where

$$C_{\psi^1\psi^2} \;\triangleq\; \int_{-\infty}^{\infty} \overline{\widehat{\psi^1}(\omega)}\, \widehat{\psi^2}(\omega)\, \frac{d\omega}{|\omega|} \;. \qquad (D.2)$$

If we abuse the requirement that s^2 be L^2 (which can be justified if we consider s^2 to be a distribution) and take $s^2(\tau) = \delta(t-\tau)$, then (D.1) yields

$$s^1(t) \;=\; \frac{1}{C_{\psi^1\psi^2}} \int_{-\infty}^{\infty} \frac{da}{a^2} \int_{-\infty}^{\infty} db \; <s^1,\, {\psi^1}_b^a> {\psi^2}_b^a(t) \;. \qquad (D.3)$$

If $\psi^2 = \psi^1 = \psi$, (D.3) becomes the double integration inversion formula

$$s(t) \;=\; \frac{1}{C_\psi} \int_{-\infty}^{\infty} \frac{da}{a^2} \int_{-\infty}^{\infty} db \; W_b^a \; \psi_b^a(t) \;, \qquad (D.4)$$

where $C_\psi \;\triangleq\; C_{\psi\psi}$ and $W_b^a = <s,\, \psi_b^a>$. Relation (D.4) differs from (1.5) inasmuch as it includes negative values of a (see below). Similarly, if $\psi^2(t) = \delta(t)$ we obtain the single integration formula. It is clear that (D.2) becomes $\int \overline{\widehat{\psi}}\, |\omega|^{-1}\, d\omega = C_{1\psi}$ of equation (4.16), and since

$$\int f(b)\, \frac{1}{\sqrt{a}}\, \delta\left(\frac{t-b}{a}\right) db \;=\; \sqrt{|a|}\, f(t) \;,$$

(D.3) becomes

$$\begin{aligned} s^1(t) \;&=\; \frac{1}{C_{1\psi}} \int_{-\infty}^{\infty} \frac{da}{|a|^{3/2}} <s^1,\, \psi_t^a> \\ &=\; \frac{1}{C_{1\psi}} \int_{-\infty}^{\infty} \frac{da}{|a|^{3/2}}\, W^a(t) \;. \end{aligned} \qquad (D.5)$$

Formulae for $a > 0$

We consider formulae for positive a. Let us write LHS_{a+} for the integral of the left hand side of (D.1), but with a restricted to $[0,\, \infty]$. The derivation in [3] yields

$$LHS_{a+} \;=\; \int_{-\infty}^{\infty} d\omega\; \widehat{s^1}(\omega)\, \overline{\widehat{s^2}(\omega)} \int_0^{\infty} \frac{da}{|a|}\, \overline{\widehat{\psi^1}(a\omega)}\, \widehat{\psi^2}(a\omega) \;. \qquad (D.6)$$

In order to render the second integral independent of ω through the substitution $a' = a\omega$, we need to have $\int_0^\infty \overline{\widehat{\psi^1}(a)}\widehat{\psi^2}(a)|a|^{-1}da = \int_0^\infty \overline{\widehat{\psi^1}(-a)}\widehat{\psi^2}(-a)|a|^{-1}da$. This will hold true, for example, when ψ^1 and ψ^2 are equal and real. In that case, the result is

$$\int_0^\infty \frac{da}{a^2} \int_{-\infty}^\infty db \; < s^1,\, \psi_b^a > < \psi_b^a,\, s^2 > \;=\; \frac{1}{2} C_\psi < s^1,\, s^2 > \quad with\ \psi\ real\ . \qquad (D.7)$$

We observe that (D.7) is a Planchere-type formula stating that the wavelet transformation $s \longrightarrow (2/C_\psi)^{1/2}\, W_b^a$ preserves inner products.

Let

$$C^+_{\psi^1\psi^2} \;\triangleq\; \int_0^\infty \overline{\widehat{\psi^1}(\omega)}\, \widehat{\psi^2}(\omega)\, \frac{d\omega}{|\omega|}\ , \qquad (D.8a)$$

$$C^-_{\psi^1\psi^2} \;\triangleq\; \int_{-\infty}^0 \overline{\widehat{\psi^1}(\omega)}\, \widehat{\psi^2}(\omega)\, \frac{d\omega}{|\omega|}\ , \qquad (D.8b)$$

$$< s^1,\, s^2 >^+ \;\triangleq\; \int_0^\infty d\omega\ \widehat{s^1}\, \overline{\widehat{s^2}}\ , \qquad (D.9a)$$

$$< s^1,\, s^2 >^- \;\triangleq\; \int_{-\infty}^0 d\omega\ \widehat{s^1}\, \overline{\widehat{s^2}}\ . \qquad (D.9b)$$

Then (D.6) may be rewritten

$$LHS_{a^+} \;=\; C^+_{\psi^1\psi^2} < s^1,\, s^2 >^+ \;+\; C^-_{\psi^1\psi^2} < s^1,\, s^2 >^-\ . \qquad (D.10)$$

If s^1 or s^2 is analytic, then $< s^1,\, s^2 >^- = 0$ and $< s^1,\, s^2 > = < s^1,\, s^2 >^+$ so that

$$< s^1,\, s^2 > \;=\; \frac{1}{C^+_{\psi^1\psi^2}} \int_0^\infty \frac{da}{a^2} \int_{-\infty}^\infty db \; < s^1,\, \psi^{1\,a}_b > < \psi^{2\,a}_b,\, s^2 > \ . \qquad (D.11)$$

If ψ^1 or ψ^2 is analytic then $C^-_{\psi^1\psi^2} = 0$ and $C_{\psi^1\psi^2} = C^+_{\psi^1\psi^2}$ so

$$< s^1,\, s^2 >^+ \;=\; \frac{1}{C_{\psi^1\psi^2}} \int_0^\infty \frac{da}{a^2} \int_{-\infty}^\infty db \; < s^1,\, \psi^{1\,a}_b > < \psi^{2\,a}_b,\, s^2 > \ . \qquad (D.12)$$

Finally, if in addition to the analyticity of ψ^1 or ψ^2, s^1 and s^2 are both real, we have $< s^1,\, s^2 >^- = \overline{< s^1,\, s^2 >^+}$ so that (D.12) becomes

$$< s^1,\, s^2 > \;=\; Re\left\{ \frac{2}{C_{\psi^1\psi^2}} \int_0^\infty \frac{da}{a^2} \int_{-\infty}^\infty db \; < s^1,\, \psi^{1\,a}_b > < \psi^{2\,a}_b,\, s^2 > \right\}\ . \qquad (D.13)$$

Taking $\psi^1 = \psi^2 = \psi$ in the above formulae, as well as $s^2(\tau) = \delta(t - \tau)$, we obtain the inversion formulae

$$s(t) = \frac{2}{C_\psi} \int_0^\infty \frac{da}{a^2} \int_{-\infty}^\infty db\ W_b^a\ \psi_b^a(t) \quad real\ \psi \tag{D.14}$$

$$s(t) = \frac{2}{C_\psi}\ Re \int_0^\infty \frac{da}{a^2} \int_{-\infty}^\infty db\ W_b^a\ \psi_b^a(t) \quad real\ s,\ analytic\ \psi \tag{D.15}$$

$$s(t) = \frac{1}{C_\psi^+} \int_0^\infty \frac{da}{a^2} \int_{-\infty}^\infty db\ W_b^a\ \psi_b^a(t) \quad analytic\ s\ . \tag{D.16}$$

To get the single integration formulae, we take $\psi^2(t) = \delta(t)$ in (D.6) obtaining

$$\int_0^\infty \frac{da}{|a|^{3/2}} \int_{-\infty}^\infty db < s^1,\ \psi_b^a > \overline{s^2(b)} = \int_{-\infty}^\infty d\omega\ \hat{s}^1(\omega)\ \overline{\hat{s}^2(\omega)} \int_0^\infty \frac{da}{|a|}\ \overline{\hat{\psi}(a\omega)}\ . \tag{D.17}$$

Defining

$$C_{1\psi}^+ \triangleq \int_0^\infty \overline{\hat{\psi}(\omega)}\ \frac{d\omega}{|\omega|} \tag{D.18}$$

and $C_{1\psi}^-$ similarly, we have

$$\int_0^\infty \frac{da}{|a|^{3/2}} \int_{-\infty}^\infty db < s^1,\ \psi_b^a > \overline{s^2(b)} = C_{1\psi}^+ < s^1,\ s^2 >^+ + C_{1\psi}^- < s^1,\ s^2 >^-\ . \tag{D.19}$$

If either s^1 or s^2 is analytic, this yields

$$< s^1,\ s^2 > = \frac{1}{C_{1\psi}^+} \int_0^\infty \frac{da}{|a|^{3/2}} \int_{-\infty}^\infty db < s^1,\ \psi_b^a > \overline{s^2(b)} \quad with\ s^1\ or\ s^2\ analytic\ . \tag{D.20}$$

If ψ is analytic

$$< s^1,\ s^2 >^+ = \frac{1}{C_{1\psi}} \int_0^\infty \frac{da}{|a|^{3/2}} \int_{-\infty}^\infty db < s^1,\ \psi_b^a > \overline{s^2(b)} \quad with\ \psi\ analytic\ . \tag{D.21}$$

If s^1 and s^2 are real, and $\hat{\psi}(\omega)$ is real, then $C_{1\psi}^+$ and $C_{1\psi}^-$ are real so that

$$LHS + \overline{LHS} = (C_{1\psi}^+ + C_{1\psi}^-) < s^1,\ s^2 >\ . \tag{D.22}$$

This yields

$$< s^1,\ s^2 > = \frac{2}{C_{1\psi}}\ Re \int_0^\infty \frac{da}{|a|^{3/2}} \int_{-\infty}^\infty db < s^1,\ \psi_b^a > \overline{s^2(b)} \quad with\ real\ s^1,\ s^2,\ \hat{\psi}\ . \tag{D.23}$$

The corresponding inversion formulae are

$$s(t) = \frac{2}{C_{1\psi}} Re \int_0^\infty \frac{da}{|a|^{3/2}} < s,\ \psi_t^a > \quad real\ s,\ real\ \widehat{\psi}(\omega) \tag{D.24}$$

$$s(t) = Re\left\{ \frac{2}{C_{1\psi}} \int_0^\infty \frac{da}{|a|^{3/2}} < s,\ \psi_t^a > \right\} \quad real\ s,\ analytic\ \psi \tag{D.25}$$

$$s(t) = \frac{1}{C_{1\psi}^+} \int_0^\infty \frac{da}{|a|^{3/2}} < s,\ \psi_t^a > \quad analytic\ s\ . \tag{D.26}$$

Note that in (D.25), $C_{1\psi}$ is generally complex. Also, there seems to be no simple single integration formula for real $s(t)$ with real $\psi(t)$.

APPENDIX E. DERIVATION OF (5.19) and(5.20)

In this appendix, it is convenient as well as enlightening to base our derivations on an alternative implementation to that found in figure 2; one which, despite appearances, is more directly related to the decimated transform of figure 1. Since $w_0^i = w_{i,0}$, and since $\mathbf{w}^i$ is translation invariant, one may compute the undecimated DWT, w_n^i, by translating the signal by n and then computing $w_{i,0}$ (cf. (2.9)). This may be efficiently implemented by the structure pictured in figure 5 [2]. This diagram is most easily visualized as 2^M copies of figure 1. The even and odd branches represent a splitting of the time series into its even and odd samples. Each horizontal path through the diagram is identical to a decimated DWT filter bank, and represents a time advance of the signal by $\sum_i 2^i \epsilon_i$ where ϵ_i is 1 for odd branches and 0 for even branches. A given path gets repeated every 2^M samples. If we index the paths by r, we see that as r goes from 0 to $2^i - 1$, the paths correspond to the sets of wavelet coefficients $\mathbf{w}_i(r)$.

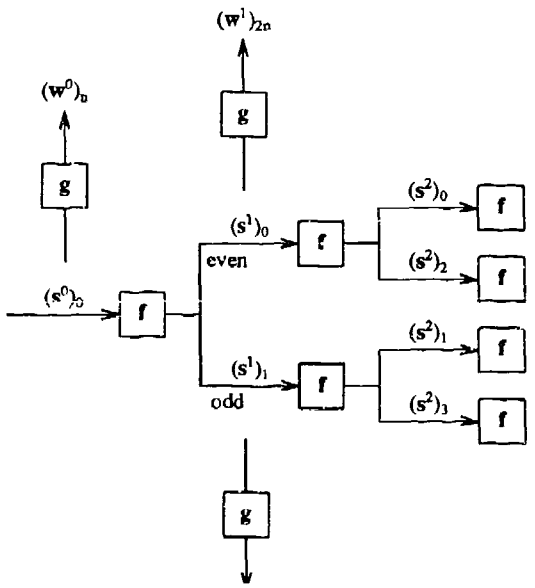

Figure 5. Implementation of undecimated wavelet transform by multiplexing decimated transforms.

The implementation of the DWT^{-1} corresponding to figure 5, is obtained by simply inverting its data flow. In this direction, the outputs of the filters $\widetilde{f}$ and $\widetilde{g}$ are summed while the junctures of even and odd branches are to be interpreted as multiplexing the two time series. This multiplexing can be represented by inserting a zero in between the samples of each channel, delaying the odd channel by one, and adding the two channels. The insertions are equivalent to applying the dilation operator $\mathbf{D}$. This accounts for the delay difference of one sample between adjacent channels resulting, ultimately, in a delay of r samples for path r relative to path 0. At octave i, $\widetilde{f} * \mathbf{D}$ will be repeated i times producing

a contribution at time m of the form $[(\widetilde{f} * \mathbf{D})^i \widetilde{g} * \mathbf{w}_i(r)]_{m-r}$ from path r. Adding these contributions, we find

$$\widetilde{s}_m \;=\; \sum_{i=0}^{M-1} \sum_{r=0}^{2^i-1} [(\widetilde{f} * \mathbf{D})^i \, (\widetilde{g} * \mathbf{w}_i(r))]_{m-r} \;+\; \sum_{r=0}^{2^M-1} [(\widetilde{f} * \mathbf{D})^M \, \mathbf{s}^M(r)]_{m-r} \;. \qquad (E.1)$$

This is equation (5.19). To prove that it actually computes the DWT^{-1}, we must demonstrate its equivalence to (5.6).

Let us take the z-transform of (E.1). We first observe that

$$\sum_k \mathrm{w}_k^i z^{-k} \;=\; \sum_{r=0}^{2^i-1} \sum_n \mathrm{w}_{2^i n+r}^i z^{-2^i n-r} \;=\; \sum_{r=0}^{2^i-1} \sum_n z^{-r} \mathrm{w}_{i,n}(r) z^{-2^i n} \;, \qquad (E.2)$$

which yields

$$\mathbf{w}_z^i(\omega) \;=\; \sum_{r=0}^{2^i-1} z^{-r} \mathbf{w}_i(r)_z(2^i\omega) \;. \qquad (E.3)$$

Also, one has, for arbitrary vectors $\mathbf{x}$ and $\mathbf{y}$,

$$(\mathbf{y} * \mathbf{D}x)_z \;=\; \mathbf{y}_z(\omega)\, \mathbf{x}_z(2\omega) \;. \qquad (E.4)$$

Repeating this i times, we find

$$\begin{aligned} [(\mathbf{y} * \mathbf{D})^i \mathbf{x}]_z \;&=\; \prod_{j=0}^{i-1} \mathbf{y}_z(2^j\omega)\, \mathbf{x}_z(2^i\omega) \\ &=\; \prod_{j=0}^{i-1} (\mathbf{D}^j \mathbf{y})_z(\omega)\, \mathbf{x}_z(2^i\omega) \;. \end{aligned} \qquad (E.5)$$

Substituting $\widetilde{g} * \mathbf{w}_i(r)$ for $\mathbf{x}$, $\widetilde{f}$ for $\mathbf{y}$, and summing over r, we obtain

$$\begin{aligned} \sum_{r=0}^{2^i-1} z^{-r} [(\widetilde{f} * \mathbf{D})^i (\widetilde{g} * \mathbf{w}_i(r))]_z \;&=\; \sum_{r=0}^{2^i-1} z^{-r} \prod_{j=0}^{i-1} (\mathbf{D}^j \widetilde{f})_z(\omega)\, \widetilde{g}_z(2^i\omega)\, \mathbf{w}_i(r)_z(2^i\omega) \\ &=\; \prod_{j=0}^{i-1} (\mathbf{D}^j \widetilde{f})_z(\omega)\, (\mathbf{D}^i \widetilde{g})_z\, \mathbf{w}_z^i(\omega) \;. \end{aligned} \qquad (E.6)$$

This is the z-transform of the contribution of $\mathbf{w}^i$ to $\widetilde{\mathbf{s}}$ (cf., (5.6)). Summing over octaves and including the DC term, we obtain equation (5.6); that is, the algorithm of figure 2b. This proves (5.19). To complete the derivation of (5.20), we note that $[\boldsymbol{g}^\dagger * \mathbf{x}]_m = \sum_n \psi(m-n) x_n$. Replacing ψ in (5.18) by $\psi'(t) \;\triangleq\; \sum_n x_n \psi(t-n)$ and $\boldsymbol{g}$ in (5.18) by $\boldsymbol{g}' \;\triangleq\; \boldsymbol{g}^\dagger * \mathbf{x}$ where $[\boldsymbol{g}']_m = \psi'(m)$, we have

$$[(\boldsymbol{f} * \mathbf{D})^i (\boldsymbol{g}^\dagger * \mathbf{x})]_m \;\approx\; \sum_n \frac{1}{\sqrt{2^i}} \psi\left(\frac{m}{2^i} - n\right) x_n \;=\; \sum_n \psi_{i,n} x_n \;. \qquad (E.7)$$

REPORT DOCUMENTATION PAGE

Form Approved
OMB No. 0704-0188

1. AGENCY USE ONLY (Leave blank)	2. REPORT DATE	3. REPORT TYPE AND DATES COVERED
	September 1993	Final

4. TITLE AND SUBTITLE

AN INVERSE DWT FOR NONORTHOGONAL WAVELETS

5. FUNDING NUMBERS

PE: 0601153N
WU: DN303036

6. AUTHOR(S)

M. J. Shensa

7. PERFORMING ORGANIZATION NAME(S) AND ADDRESS(ES)

Naval Command, Control and Ocean Surveillance Center (NCCOSC)
RDT&E Division
San Diego, CA 92152-5230

8. PERFORMING ORGANIZATION REPORT NUMBER

TR 1621

9. SPONSORING/MONITORING AGENCY NAME(S) AND ADDRESS(ES)

Office of Naval Research
800 N. Quincy St.
Arlinton, VA 22217

10. SPONSORING/MONITORING AGENCY REPORT NUMBER

11. SUPPLEMENTARY NOTES

12a. DISTRIBUTION/AVAILABILITY STATEMENT

Approved for public release; distribution is unlimited.

12b. DISTRIBUTION CODE

13. ABSTRACT *(Maximum 200 words)*

Discrete nonorthogonal wavelet transforms play an important role in signal processing by offering finer resolution in time and scale than their orthogonal counterparts. The standard inversion procedure for such transforms is a finite expansion in terms of the analyzing wavelet. This approximation works quite well for many signals; however, for other signals, it fails to achieve good accuracy or requires an excessive number of scales. This paper proposes several algorithms that provide more adequate inversion and compares them in the case of Morlet wavelets. In the process, both practical and theoretical issues for the inversion of nonorthogonal wavelet transforms are discussed.

14. SUBJECT TERMS

nonorthogonal wavelet transforms
dual wavelets

15. NUMBER OF PAGES

59

16. PRICE CODE

17. SECURITY CLASSIFICATION OF REPORT	18. SECURITY CLASSIFICATION OF THIS PAGE	19. SECURITY CLASSIFICATION OF ABSTRACT	20. LIMITATION OF ABSTRACT
UNCLASSIFIED	UNCLASSIFIED	UNCLASSIFIED	SAME AS REPORT

21a. NAME OF RESPONSIBLE INDIVIDUAL	21b. TELEPHONE *(Include Area Code)*	21c. OFFICE SYMBOL
M. J. Shensa	(619) 553–5702	Code 782

INITIAL DISTRIBUTION (U)

Code 0012	Patent Counsel	(1)
Code 02712	Archive/Stock	(6)
Code 0274B	Library	(2)
Code 014	K. Campell	(1)
Code 0141	A. Grodon	(1)
Code 70	T. F. Ball	(1)
Code 75	J. E. Griffin	(1)
Code 755	R. J. Dinger	(1)
Code 755	M. Pollock	(1)
Code 761	D. Stein	(1)
Code 78	P. M. Reeves	(1)
Code 782	M. J. Shensa	(30)
Code 824	R. North	(1)

Defense Technical Information Center
Alexandria, VA 22304–6145 (4)

NCCOSC Washington Liaison Office
Washington, DC 20363–5100

Center for Naval Analyses
Alexandria, VA 22302–0268

Navy Acquisition, Research & Development
Information Center (NARDIC)
Washington, DC 20360–5000

GIDEP Operations Center
Corona, CA 91718–8000

NCCOSC Division Detachment
Warminster, PA 18974–5000

Navy Personnel Research & Development
Center
San Diego, CA 92152–6800

Office of Naval Research
Arlington, VA 22217–5000

Naval Air Warfare Center
Weapons Division
China Lake, CA 93555–6001 (3)

National Institute of Health
Bethesda, MD 20892 (2)

ATT
Murray Hill, NJ 07974-0636

University of Maryland
College Park, MD 20742 (2)

University of Minnesota
Minneapolis, MN 55455

New York University
Courant Institute of Mathematical Sciences
New York, NY 10012

Pennsylvania State University
Applied Research Laboratory
State College, PA 16804

Rutgers University
New Brunswick, NJ 08903

Stanford University
Stanford, CA 94305

Schlumberger-Doll Research
Ridgefield, CT 06877–4108